

Controlling and Predicting Alkyl-Onium Electronic Structure

Frances K. Towers Tompkins,^a Lewis G. Parker,^a Richard M. Fogarty,^b Jake M. Seymour,^a Ekaterina Gousseva,^a David C. Grinter,^c Robert G. Palgrave,^d Christopher D. Smith,^a Roger A Bennett,^a Richard P. Matthews,^e Kevin R. J. Lovelock^a

^a Department of Chemistry, University of Reading, UK

^b Department of Chemistry, Imperial College London, UK

^c Diamond Light Source, UK

^d Department of Chemistry, University College London, UK

^e Department of Biosciences, University of East London, UK

* k.r.j.lovelock@reading.ac.uk

† R.Matthews3@uel.ac.uk

1. XPS experiments: methods	S2
2. DFT calculations: methods	S3-S4
3. Ionic liquids and cations studied	S5-S10
4. Data analysis. Peak fitting core level XP spectra	S11
5. Data analysis. Charge referencing and area normalisation	S12-S13
6. Results. XPS: demonstrating purity	S14-S30
7. Results. Experimental and calculated $E_B(X \text{ core})$	S31-S33
8. Results. Experimental N 1s XP spectra: effect of $[\text{FSI}]^-$ versus $[\text{NTf}_2]^-$	S34
9. Results. Experimental versus calculated N 1s XP spectra	S35-S36
10. Results. Effect of SMD parameters/gas-phase on N 1s XP spectra	S37
11. Results. Linear correlations of calculated versus experimental $E_B(\text{N}_{\text{cation}} \text{ 1s})$	S38
12. Results. Calculated P 2p XPS	S39
13. Effect of branching alkyl chains	S40
14. Results. C 1s comparisons	S41-S44
15. References	S45

1. XPS experiments: methods

Laboratory-based XPS was recorded for five ILs ($[N_{8,8,8,1}][NTf_2]$, $[C_8C_1Pyrr][NTf_2]$, $[N_{4,1,1,1}][FSI]$, $[N_{4,4,4,1}][FSI]$, $[P_{i4,1,1,1}][NTf_2]$) at the University of Reading on a Thermo Scientific ESCALAB 250 monochromated Al K α source ($h\nu = 1486.6$ eV) spectrometer. A drop of IL was placed directly onto a stainless steel sample plate. This sample was placed in a loadlock and the pressure reduced to 10^{-7} mbar by pumping down for > 6 hours. After attaining the required pressure, the IL was transferred to the analysis chamber. For $[N_{8,8,8,1}][NTf_2]$, $[N_{4,1,1,1}][FSI]$ and $[P_{i4,1,1,1}][NTf_2]$ an area scan was performed to minimise sample charging/damage. Acquisition parameters were matched to give comparable energy resolution with data already published; a pass energy of 20 eV was used for core-levels.

Laboratory-based XPS was recorded for one IL ($[N_{4,2,2,2}][NTf_2]$) at University College London on a Thermo Scientific Theta Probe monochromated Al K α source ($h\nu = 1486.6$ eV) spectrometer. A drop of IL was placed directly onto a stainless steel sample plate. This sample was placed in a loadlock and the pressure reduced to 10^{-7} mbar by pumping down for > 6 hours. After attaining the required pressure, the IL was transferred to the analysis chamber. Etching was carried out using a 500 eV Ar $^+$ ion beam for 10 minutes. Charge compensation was achieved using a dual beam flood gun which applied both electrons and low energy Ar $^+$ ions to the sample. Acquisition parameters were matched to give comparable energy resolution with data already published; a pass energy of 20 eV was used for core-levels.

Synchrotron-based XPS was recorded for eight ILs ($[N_{4,2,2,2}][NTf_2]$, $[N_{8,2,2,2}][NTf_2]$, $[N_{4,4,4,1}][NTf_2]$, $[C_4C_1Pip][NTf_2]$, $[N_{3,1,1,1}][NTf_2]$, $[N_{4,1,1,1}][NTf_2]$, $[N_{6,1,1,1}][NTf_2]$, $[N_{4,4,4,1}][FSI]$) at beamline B07-B XPS.¹ A drop of IL was placed directly onto a custom-made tantalum sample plate. This sample was placed in a loadlock and the pressure reduced to 10^{-7} mbar by pumping down for > 6 hours. After attaining the required pressure, the IL was transferred to the analysis chamber. Rastering of the sample was performed to minimise sample charging/damage. Acquisition parameters were matched to give comparable energy resolution with data already published; a pass energy of 20 eV was used for core-levels.

Laboratory-based XP spectra have already been published for four ILs ($[N_{3,2,1,1}][NTf_2]$, $[N_{4,1,1,1}][NTf_2]$, $[S_{2,2,1}][NTf_2]$, $[S_{2,2,2}][NTf_2]$).² $E_B(\text{core})$ are published here for the first time for these four ILs.

All experimental XP spectra were fitted using CASAXPSTM software. Fitting was carried out using a Shirley background and GL30 line shapes (70% Gaussian, 30% Lorentzian). Peak constraints used are outlined in the ESI Section 4. Relative sensitivity factors (RSFs) from ref³ were used to ensure the experimental stoichiometries matched the nominal stoichiometries. RSF values for XPS recorded on beamline B07-B at Diamond Light Source were estimated using the nominal stoichiometries; the dipole anisotropy parameter, β , was not taken into account for these RSF values.

The IL XPS measurements were made under ultrahigh vacuum (UHV) conditions. These UHV conditions mean that residual molecular solvents will have vaporized prior to XPS measurements, giving ultrapure samples from a molecular solvent contamination perspective. Furthermore, the element-specific nature of XPS means that a number of ionic impurities, *e.g.* Na $^+$, can be observed if present (see ESI Section 6). Therefore, we can have very high confidence in the purity of our ILs for the XPS measurements.

2. DFT calculations: methods

All DFT calculations were carried out using Gaussian 16 (version C.01).⁴ Each of the onium species were optimised under no symmetry constraints and confirmed as minima using vibrational analysis. The long-range corrected ω B97XD functional^{5, 6} was employed in conjunction with the quadruple zeta def2-QZVPP basis set.^{7, 8} The SMD (Solvation Model based on Density) was employed account for IL solvent effects. Specifically, the [C₄C₁Im][PF₆] parameters (relative permittivity, ϵ_r , = 11.40; refractive index, n , = 1.4090; surface tension, γ , = 0.266 cal mol⁻¹ Å²; Abraham basicity, β , = 0.216)⁹ were selected to be consistent with previous ionic liquid work.¹⁰ The SMD water solvent continuum was employed for calculations in water solvent.

For calculations in both gas-phase and implicit solvent, optimisation convergence criteria were set to 10⁻¹¹ on the density matrix and 10⁻⁹ on the energy matrix. Moreover, the numerical grid was improved from the default using the “int=SuperFineGrid” keyword. Vibrational frequencies and zero-point vibrational energy corrections (ZPE) were attained using the harmonic approximation.

In this work, for both gas-phase and implicit solvent cations, binding energies (E_B) were determined using Koopmans' theorem which states that the ionisation energy of molecular species is equal to the negative of the orbital energy ($E_B = -E$).¹¹⁻¹³ This approximation, while crude, is easily accessible by standard computational approaches and fits very well with experimental data with the inclusion of an explicit solvent environment. It should also be noted that this approach works specifically well when there are no significant final state effects (or when final state effects are constant). This means that this method can give a useful guide to evaluate the trends in initial state effects which are of inductive type and caused by the electron density over the atomic site where core ionization occurs. However, the method is highly dependent on the accuracy of the method (HF or DFT functional) and on the choice of basis-set. Our selection of the ω B97XD functional was made based on reduced self-interaction error compared to conventional hybrid GGA (generalised gradient approximation) functionals and the quadruple zeta def2-QZVPP basis set was selected based on recent work.^{10, 14}

To produce calculated XP spectra for orbitals that have spin-orbit coupling (S 2p, P 2p), each calculated E_B value was adjusted using E_B and area factors are given in Table S1. Once the adjusted calculated E_B were obtained, a Gaussian-Lorentzian Product (GLP) function was applied to each calculated E_B data point for each core-state using Equation 1 and then summed to produce calculated XPS data. The mixing parameter, m , and function width, F , were set to the values given in Table S1.

To produce calculated XP spectra for orbitals that do not have spin-orbit coupling (N 1s, C 1s), a Gaussian-Lorentzian Product (GLP) function was applied to each calculated E_B data point for each valence-state using Equation 1 and then summed to produce calculated XPS data. The mixing parameter, m , and function width, F , were set to the values given in Table S1.

$$GLP(x; F, E, m) = \frac{\exp\left[-4 \ln 2(1-m)\frac{(x-E)^2}{F^2}\right]}{\left[1+4m\frac{(x-E)^2}{F^2}\right]} \quad (\text{Equation 1})$$

Table S1. Values used to produce calculated XP spectra

Orbital	function width, F / eV	Gaussian-Lorentzian (GL) Product function	Spin-orbit coupling ΔE_B / eV	$E_B(\text{calc.})$ with spin-orbit coupling correction	Spin-orbit coupling peak area ratio	Peak area ratio
N 1s	1.05	GL(30)	N/A	N/A	N/A	N/A
C 1s	1.10	GL(30)	N/A	N/A	N/A	N/A
S 2p	1.05	GL(30)	$\Delta E_B(\text{S } 2p_{3/2} - \text{S } 2p_{1/2}) = 1.20 \text{ eV}$	$E_B(\text{S } 2p_{3/2}, \text{calc.}) = E_B(\text{S } 2p, \text{calc.}) - (1.20 \times 2/3)$	1:2 for $2p_{1/2}:2p_{3/2}$	$\text{Area}(\text{S } 2p_{3/2}, \text{calc.}) = \text{Area}(\text{S } 2p, \text{calc.}) \times 2/3$
				$E_B(\text{S } 2p_{1/2}, \text{calc.}) = E_B(\text{S } 2p, \text{calc.}) + (1.20 \times 1/3)$		$\text{Area}(\text{S } 2p_{1/2}, \text{calc.}) = \text{Area}(\text{S } 2p, \text{calc.}) \times 1/3$
P 2p	1.05	GL(30)	$\Delta E_B(\text{P } 2p_{3/2} - \text{P } 2p_{1/2}) = 0.87 \text{ eV}$	$E_B(\text{P } 2p_{3/2}, \text{calc.}) = E_B(\text{P } 2p, \text{calc.}) - (0.87 \times 2/3)$	1:2 for $2p_{1/2}:2p_{3/2}$	$\text{Area}(\text{P } 2p_{3/2}, \text{calc.}) = \text{Area}(\text{P } 2p, \text{calc.}) \times 2/3$
				$E_B(\text{P } 2p_{1/2}, \text{calc.}) = E_B(\text{P } 2p, \text{calc.}) + (0.87 \times 1/3)$		$\text{Area}(\text{P } 2p_{1/2}, \text{calc.}) = \text{Area}(\text{P } 2p, \text{calc.}) \times 1/3$

3. Ionic liquids and cations studied

3.1. XPS experiments: ionic liquids studied

Ionic liquids were purchased from Iolitec or Solvionic (Table S2) and used as received. Sample purity was confirmed by XP survey spectra (ESI Section 6).

Table S2. ILS investigated using X-ray photoelectron spectroscopy (XPS) in this work

IL no.	Abbreviation	Structure	Name	Ref. or bought for this work	
1	[N _{4,2,2,2}][NTf ₂]			<i>n</i> -butyl(triethyl)ammonium bis[(trifluoromethane)sulfonyl]imide	Purchased from lolitec
2	[N _{8,2,2,2}][NTf ₂]			<i>n</i> -octyl(triethyl)ammonium bis[(trifluoromethane)sulfonyl]imide	Purchased from lolitec
3	[N _{4,4,4,1}][NTf ₂]			tri- <i>n</i> -butyl(methyl)ammonium bis[(trifluoromethane)sulfonyl]imide	Purchased from lolitec
4	[N _{8,8,8,1}][NTf ₂]			tri- <i>n</i> -octyl(methyl)ammonium bis[(trifluoromethane)sulfonyl]imide	Purchased from lolitec
5	[C ₄ C ₁ Pip][NTf ₂]			1- <i>n</i> -butyl-1-methylpiperidinium bis[(trifluoromethane)sulfonyl]imide	Purchased from lolitec
6	[C ₈ C ₁ Pyrr][NTf ₂]			1- <i>n</i> -octyl-1-methylpyrrolidinium bis[(trifluoromethane)sulfonyl]imide	Purchased from lolitec
7	[N _{3,2,1,1}][NTf ₂]			<i>n</i> -propyl(ethyl)(dimethyl)ammonium bis[(trifluoromethane)sulfonyl]imide ²	
8	[N _{3,1,1,1}][NTf ₂]			<i>n</i> -propyl(trimethyl)ammonium bis[(trifluoromethane)sulfonyl]imide	Purchased from Solvionic

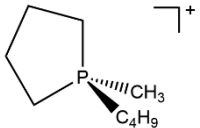
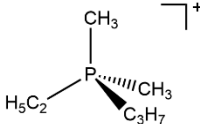
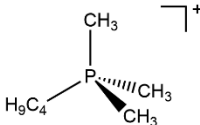
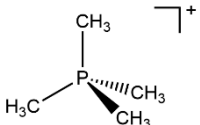
9	[N _{4,1,1,1}][NTf ₂]			<i>n</i> -butyl(trimethyl)ammonium bis[(trifluoromethane)sulfonyl]imide	² and purchased from Iolitec
10	[N _{6,1,1,1}][NTf ₂]			<i>n</i> -hexyl(trimethyl)ammonium bis[(trifluoromethane)sulfonyl]imide	Purchased from Solvionic
11	[N _{4,1,1,1}][FSI]			<i>n</i> -butyl(trimethyl)ammonium bis(fluorosulfonyl)imide	Purchased from Solvionic
12	[N _{4,4,4,1}][FSI]			tri- <i>n</i> -butyl(methyl)ammonium bis(fluorosulfonyl)imide	Purchased from Iolitec
13	[S _{2,2,1}][NTf ₂]			diethyl(methyl)sulfonium bis[(trifluoromethane)sulfonyl]imide	²
14	[S _{2,2,2}][NTf ₂]			triethylsulfonium bis[(trifluoromethane)sulfonyl]imide	²
15	[P _{i,4,1,1,1}][NTf ₂]			<i>i</i> -butyl(trimethyl)phosphonium bis[(trifluoromethane)sulfonyl]imide	Purchased from Solvionic

3.2. DFT calculations: cations studied

Table S3. Onium cations investigated using calculations in this work

Cation no.	Abbreviation	Structure	Name
1	$[N_{i3,i3,i3,i3}]^+$		tetra- <i>iso</i> -propylammonium
2	$[N_{2,2,2,2}]^+$		tetraethylammonium
3	$[N_{4,2,2,2}]^+$		<i>n</i> -butyl(triethyl)ammonium
4	$[N_{8,2,2,2}]^+$		<i>n</i> -octyl(triethyl)ammonium
5	$[N_{2,2,2,1}]^+$		triethyl(methyl)ammonium
6	$[N_{4,4,4,1}]^+$		<i>n</i> -tributyl(methyl)ammonium
7	$[C_4C_1Pip]^+$		1-butyl-1-methylpiperidinium
8	$[C_4C_1Pyrr]^+$		1-butyl-1-methylpyrrolidinium
9	$[C_8C_1Pyrr]^+$		1-octyl-1-methylpyrrolidinium
10	$[N_{3,2,1,1}]^+$		<i>n</i> -propyl(ethyl)(dimethyl)ammonium
11	$[N_{2,2,1,1}]^+$		diethyl(dimethyl)ammonium
12	$[N_{2,1,1,1}]^+$		ethyl(trimethyl)ammonium

13	$[N_{3,1,1,1}]^+$		<i>n</i> -propyl(trimethyl)ammonium
14	$[N_{4,1,1,1}]^+$		<i>n</i> -butyl(trimethyl)ammonium
15	$[N_{6,1,1,1}]^+$		<i>n</i> -hexyl(trimethyl)ammonium
16	$[N_{8,1,1,1}]^+$		<i>n</i> -octyl(trimethyl)ammonium
17	$[N_{16,1,1,1}]^+$		<i>n</i> -hexadecyl(trimethyl)ammonium
18	$[N_{1,1,1,1}]^+$		tetramethylammonium
19	$[S_{2,2,2}]^+$		triethylsulfonium
20	$[S_{2,2,1}]^+$		diethyl(methyl)sulfonium
21	$[S_{2,1,1}]^+$		ethyl(dimethyl)sulfonium
22	$[S_{1,1,1}]^+$		trimethyl(methyl)sulfonium
23	$[P_{2,2,2,2}]^+$		tetraethylphosphonium
24	$[P_{4,2,2,2}]^+$		<i>n</i> -butyl(triethyl)phosphonium
25	$[P_{8,2,2,2}]^+$		<i>n</i> -octyl(triethyl)phosphonium
26	$[P_{4,4,4,1}]^+$		<i>n</i> -tributyl(methyl)phosphonium
27	$[C_4C_1\text{phin}]^+$		1-butyl-1-methylphosphinanium

28	$[C_4C_1phol]^+$		1-butyl-1-methylphospholanium
29	$[P_{3,2,1,1}]^+$		<i>n</i> -propyl(ethyl)(dimethyl)phosphonium
30	$[P_{4,1,1,1}]^+$		<i>n</i> -butyl(trimethyl)phosphonium
31	$[P_{1,1,1,1}]^+$		tetramethylphosphonium

4. Data analysis. Peak fitting core level XP spectra

As well as drawing conclusions on onium electronic structure, peak fitting core level XP spectra is important for charge referencing (ESI Section 5) and demonstrating purity (ESI Section 6). All core-level XP spectra were fitted using CASAXPS™ software. Spectra were fitted with a GL30 lineshape (70% Gaussian, 30% Lorentzian) and a Shirley background. How the core level XP spectra were fitted is given in Table S4, along with any constraints used.

Table S4. Fitting constraints used for core level X-ray photoelectron spectroscopy (XPS) for each ionic liquid

IL no.	Abbreviation	Core level	Fitting constraints used
1	[N _{4,2,2,2}][NTf ₂]	C 1s	4:6 for C _{hetero} :C _{alkyl}
		S 2p	1:2 for 2p _{1/2} :2p _{3/2}
2	[N _{8,2,2,2}][NTf ₂]	C 1s	4:10 for C _{hetero} :C _{alkyl}
		S 2p	1:2 for 2p _{1/2} :2p _{3/2}
3	[N _{4,4,4,1}][NTf ₂]	C 1s	4:9 for C _{hetero} :C _{alkyl}
		S 2p	1:2 for 2p _{1/2} :2p _{3/2}
4	[N _{8,8,8,1}][NTf ₂]	C 1s	4:21 for C _{hetero} :C _{alkyl}
		S 2p	1:2 for 2p _{1/2} :2p _{3/2}
5	[C ₄ C ₁ Pip][NTf ₂]	C 1s	4:6 for C _{hetero} :C _{alkyl}
		S 2p	1:2 for 2p _{1/2} :2p _{3/2}
6	[C ₈ C ₁ Pyrr][NTf ₂]	C 1s	4:9 for C _{hetero} :C _{alkyl}
		S 2p	1:2 for 2p _{1/2} :2p _{3/2}
7	[N _{3,2,1,1}][NTf ₂]	C 1s	4:3 for C _{hetero} :C _{alkyl}
		S 2p	1:2 for 2p _{1/2} :2p _{3/2}
8	[N _{3,1,1,1}][NTf ₂]	C 1s	4:2 for C _{hetero} :C _{alkyl}
		S 2p	1:2 for 2p _{1/2} :2p _{3/2}
9	[N _{4,1,1,1}][NTf ₂]	C 1s	4:3 for C _{hetero} :C _{alkyl}
		S 2p	1:2 for 2p _{1/2} :2p _{3/2}
10	[N _{6,1,1,1}][NTf ₂]	C 1s	4:5 for C _{hetero} :C _{alkyl}
		S 2p	1:2 for 2p _{1/2} :2p _{3/2}
11	[N _{4,1,1,1}][FSI]	C 1s	4:3 for C _{hetero} :C _{alkyl}
		S 2p	1:2 for 2p _{1/2} :2p _{3/2}
12	[N _{4,4,4,1}][FSI]	C 1s	4:9 for C _{hetero} :C _{alkyl}
		S 2p	1:2 for 2p _{1/2} :2p _{3/2}
13	[S _{2,2,1}][NTf ₂]	C 1s	3:2 for C _{hetero} :C _{alkyl}
		S 2p	1:2 for 2p _{1/2} :2p _{3/2}
14	[S _{2,2,2}][NTf ₂]	C 1s	3:3 for C _{hetero} :C _{alkyl}
		S 2p	1:2 for 2p _{1/2} :2p _{3/2}
15	[P _{i4,1,1,1}][NTf ₂]	C 1s	4:3 for C _{hetero} :C _{alkyl}
		S 2p	FWHM(C _{hetero}) = FWHM(C _{alkyl})
		P 2p	1:2 for 2p _{1/2} :2p _{3/2}

5. Data analysis. Charge referencing and area normalisation

In ESI Table S5, the core orbital used for charge referencing is given, which in all cases is $E_B(N_{\text{anion}} 1s)$ (Figure S1). For $[\text{NTf}_2]^-$ and $[\text{FSI}]^-$ -containing ionic liquids the peak from the nitrogen in the anion, $N_{\text{anion}} 1s$, does not overlap with the peak from the nitrogen in the tetraalkylammonium cation, $N_{\text{cation}} 1s$, which means the experimental uncertainty of $E_B(N_{\text{cation}} 1s)$ is relatively small, ± 0.03 eV (rather than the more commonly quoted experimental uncertainty of ± 0.1 eV when comparing E_B for peaks from different elements).¹⁵ The same advantage can also hold for these two anions with trialkylsulfonium cations, where $S_{\text{cation}} 2p$ and $S_{\text{anion}} 2p$ contributions do not overlap,¹⁶ although we chose to use $E_B(N_{\text{cation}} 1s)$ for charge referencing for these two ILs also.

Table S5. Experimental X-ray photoelectron spectroscopy (XPS) details on the charge correction applied for each ionic liquid, and any fitting constraints needed to fit the core orbital used for charge referencing

IL no.	Abbreviation	Charge referencing method used from reference ¹⁷	Core orbital used for charge referencing	Fitting constraints used	E_B for core orbital used for charge referencing / eV	Rationale for choosing core orbital used for charge referencing
1	$[\text{N}_{4,2,2,2}][\text{NTf}_2]$	ii	$N_{\text{anion}} 1s$	None	399.46	$N_{\text{anion}} 1s$ for $[\text{C}_n\text{C}_1\text{Im}][\text{NTf}_2]$ ¹⁸
2	$[\text{N}_{8,2,2,2}][\text{NTf}_2]$	ii	$N_{\text{anion}} 1s$	None	399.46	$N_{\text{anion}} 1s$ for $[\text{C}_n\text{C}_1\text{Im}][\text{NTf}_2]$ ¹⁸
3	$[\text{N}_{4,4,4,1}][\text{NTf}_2]$	ii	$N_{\text{anion}} 1s$	None	399.46	$N_{\text{anion}} 1s$ for $[\text{C}_n\text{C}_1\text{Im}][\text{NTf}_2]$ ¹⁸
4	$[\text{N}_{8,8,8,1}][\text{NTf}_2]$	ii	$N_{\text{anion}} 1s$	None	399.46	$N_{\text{anion}} 1s$ for $[\text{C}_n\text{C}_1\text{Im}][\text{NTf}_2]$ ¹⁸
5	$[\text{C}_4\text{C}_1\text{Pip}][\text{NTf}_2]$	ii	$N_{\text{anion}} 1s$	None	399.46	$N_{\text{anion}} 1s$ for $[\text{C}_n\text{C}_1\text{Im}][\text{NTf}_2]$ ¹⁸
6	$[\text{C}_8\text{C}_1\text{Pyrr}][\text{NTf}_2]$	ii	$N_{\text{anion}} 1s$	None	399.46	$N_{\text{anion}} 1s$ for $[\text{C}_n\text{C}_1\text{Im}][\text{NTf}_2]$ ¹⁸
7	$[\text{N}_{3,2,1,1}][\text{NTf}_2]$	ii	$N_{\text{anion}} 1s$	None	399.46	$N_{\text{anion}} 1s$ for $[\text{C}_n\text{C}_1\text{Im}][\text{NTf}_2]$ ¹⁸
8	$[\text{N}_{3,1,1,1}][\text{NTf}_2]$	ii	$N_{\text{anion}} 1s$	None	399.46	$N_{\text{anion}} 1s$ for $[\text{C}_n\text{C}_1\text{Im}][\text{NTf}_2]$ ¹⁸
9	$[\text{N}_{4,1,1,1}][\text{NTf}_2]$	ii	$N_{\text{anion}} 1s$	None	399.46	$N_{\text{anion}} 1s$ for $[\text{C}_n\text{C}_1\text{Im}][\text{NTf}_2]$ ¹⁸
10	$[\text{N}_{6,1,1,1}][\text{NTf}_2]$	ii	$N_{\text{anion}} 1s$	None	399.46	$N_{\text{anion}} 1s$ for $[\text{C}_n\text{C}_1\text{Im}][\text{NTf}_2]$ ¹⁸
11	$[\text{N}_{4,1,1,1}][\text{FSI}]$	ii	$N_{\text{anion}} 1s$	None	399.79	$N_{\text{anion}} 1s$ for $[\text{C}_8\text{C}_1\text{Im}][\text{FSI}]$ ¹⁸
12	$[\text{N}_{4,4,4,1}][\text{FSI}]$	ii	$N_{\text{anion}} 1s$	None	399.79	$N_{\text{anion}} 1s$ for $[\text{C}_8\text{C}_1\text{Im}][\text{FSI}]$ ¹⁸
13	$[\text{S}_{2,2,1}][\text{NTf}_2]$	ii	$N_{\text{anion}} 1s$	None	399.46	$N_{\text{anion}} 1s$ for $[\text{C}_n\text{C}_1\text{Im}][\text{NTf}_2]$ ¹⁸
14	$[\text{S}_{2,2,2}][\text{NTf}_2]$	ii	$N_{\text{anion}} 1s$	None	399.46	$N_{\text{anion}} 1s$ for $[\text{C}_n\text{C}_1\text{Im}][\text{NTf}_2]$ ¹⁸
15	$[\text{P}_{i4,1,1,1}][\text{NTf}_2]$	ii	$F_{\text{anion}} 1s$	None	688.79	$F_{\text{anion}} 1s$ for $[\text{P}_{6,6,6,14}][\text{NTf}_2]$

Quantitative area normalisation to aid visual interpretation of core level XP spectra is achieved by using a peak common to all ILs. For N 1s spectra, $N_{\text{anion}} 1s$ is used, with all XP spectra divided by the peak area for $N_{\text{anion}} 1s$. For C 1s spectra, $C_{\text{hetero}} 1s$ is used, with all XP spectra divided by the peak area for $C_{\text{hetero}} 1s$.

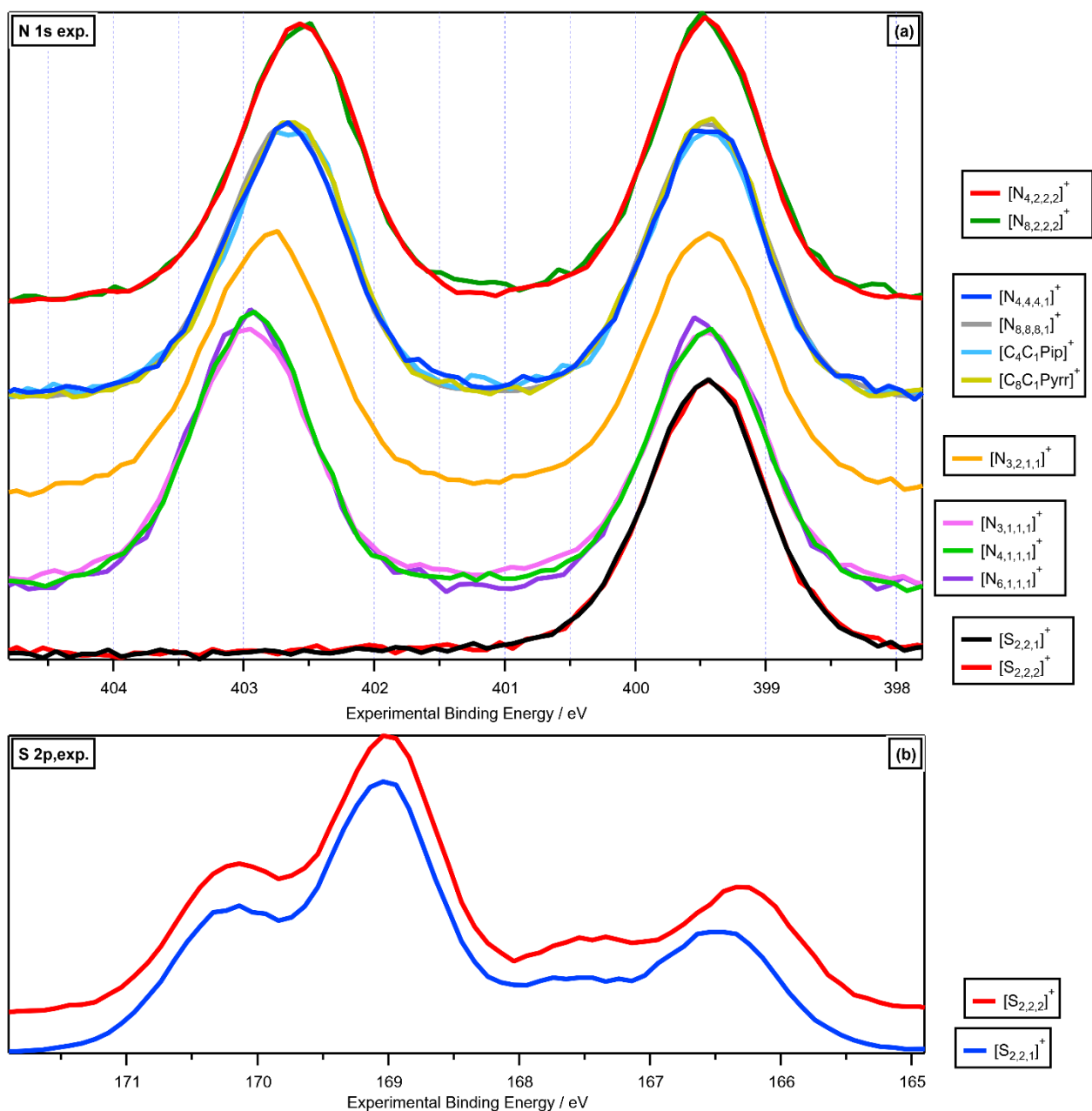


Figure S1. Experimental core XP spectra: (a) N 1s,exp. for $[N_{3,1,1,1}][NTf_2]$, $[N_{4,1,1,1}][NTf_2]$, $[N_{6,1,1,1}][NTf_2]$, $[N_{3,2,1,1}][NTf_2]$, $[N_{4,4,4,1}][NTf_2]$, $[N_{8,8,8,1}][NTf_2]$, $[C_4C_1Pip][NTf_2]$, $[C_8C_1Pyrr][NTf_2]$, $[N_{4,2,2,2}][NTf_2]$, $[N_{8,2,2,2}][NTf_2]$, $[S_{2,2,1}][NTf_2]$ and $[S_{2,2,2}][NTf_2]$; (b) S 2p,exp. for $[S_{2,2,1}][NTf_2]$ and $[S_{2,2,2}][NTf_2]$. Experimental XP spectra are area normalised and charge referenced using methods given in ESI Section 5. Traces are vertically offset for clarity.

6. Results. XPS: demonstrating purity

6.1. Results. XPS: demonstrating purity using laboratory-based XPS

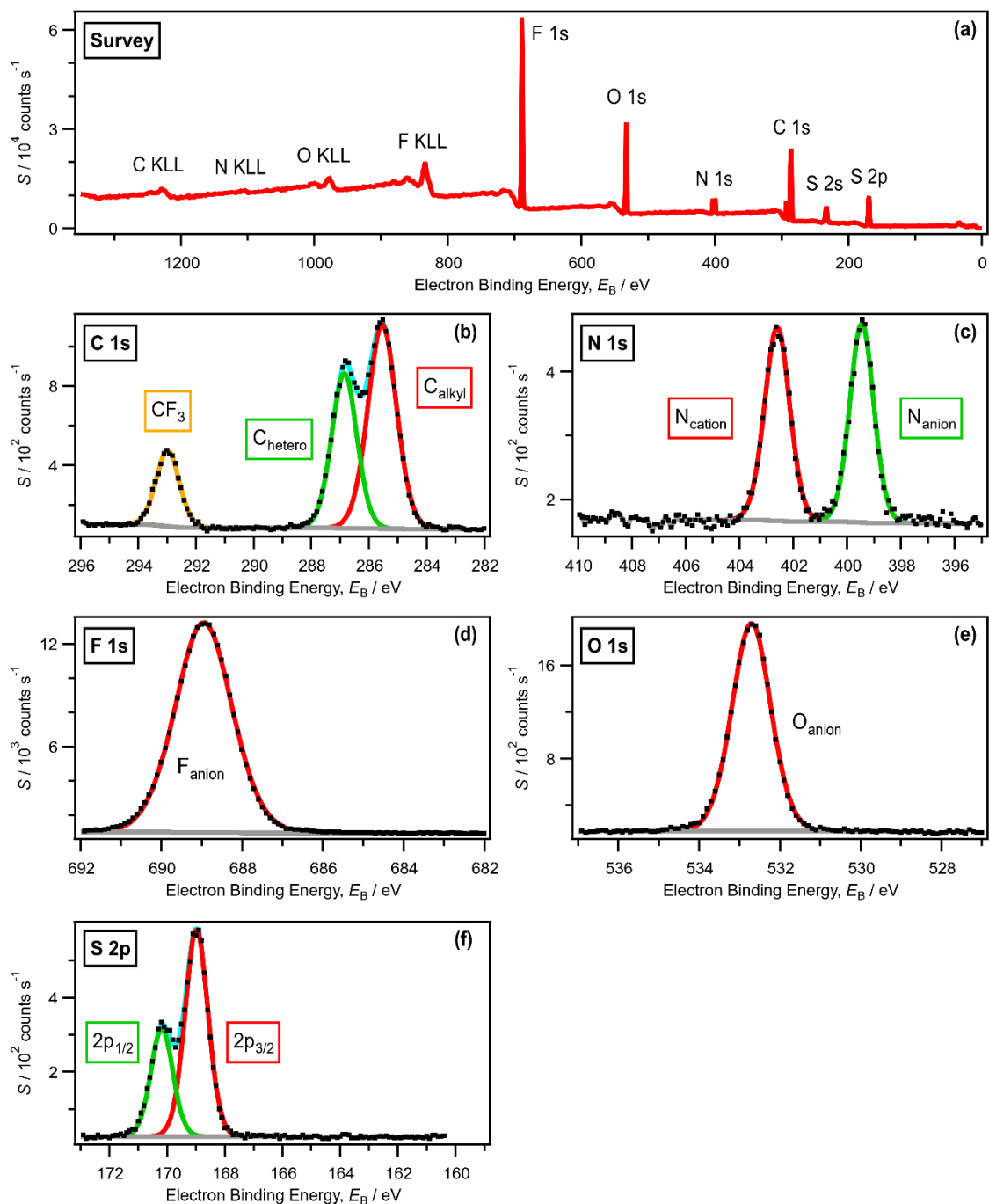


Figure S2. (a) Survey, (b-f) core XP spectra for $[N_{4,2,2,2}][NTf_2]$ recorded on laboratory-based XPS apparatus at $h\nu = 1486.6 \text{ eV}$. All XP spectra were charge referenced using the method outlined in ESI Section 5.

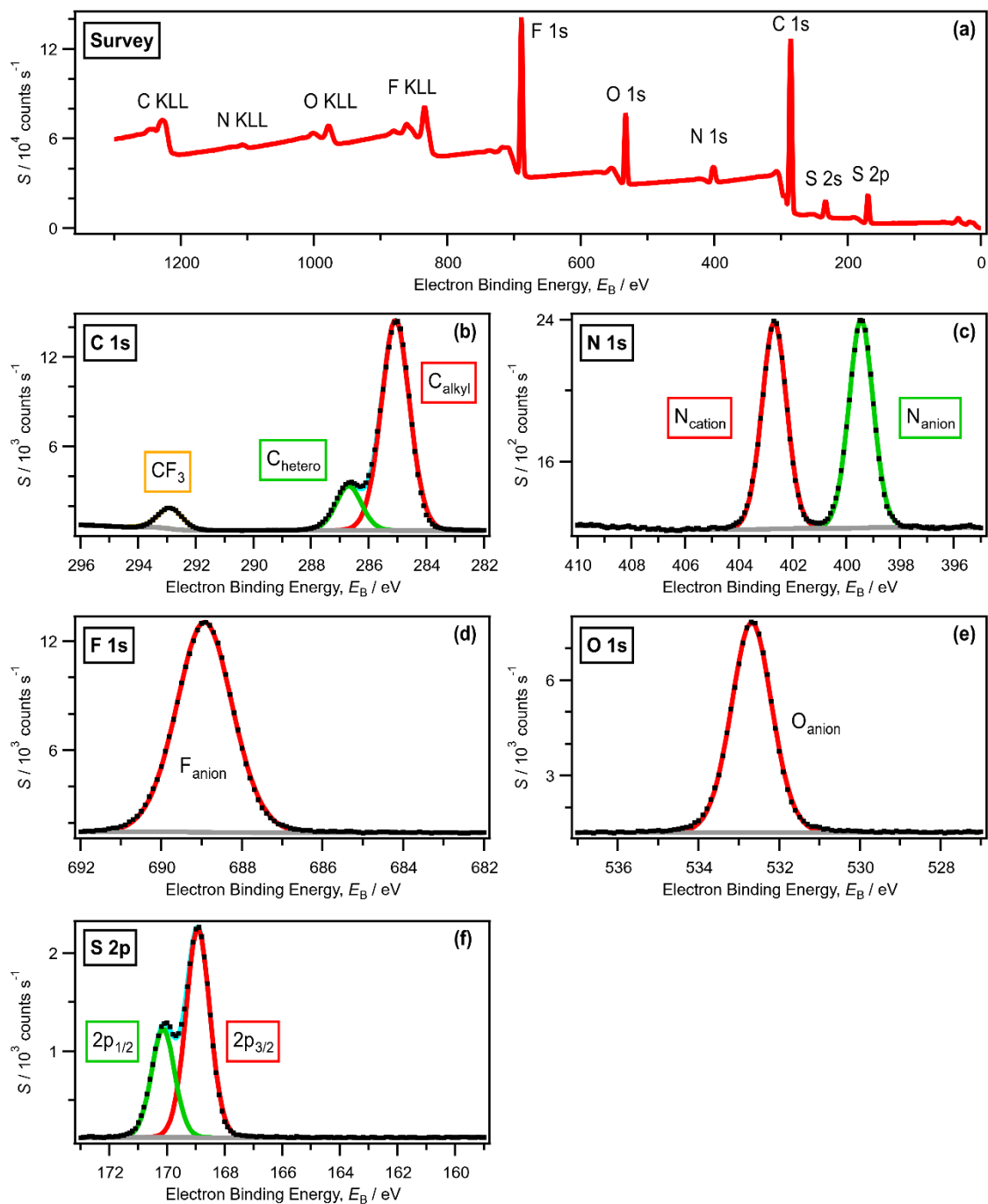


Figure S3. (a) Survey, (b-f) core XP spectra for $[N_{8,8,1}][NTf_2]$ recorded on laboratory-based XPS apparatus at $h\nu = 1486.6 \text{ eV}$. All XP spectra were charge referenced using the method outlined in ESI Section 5.

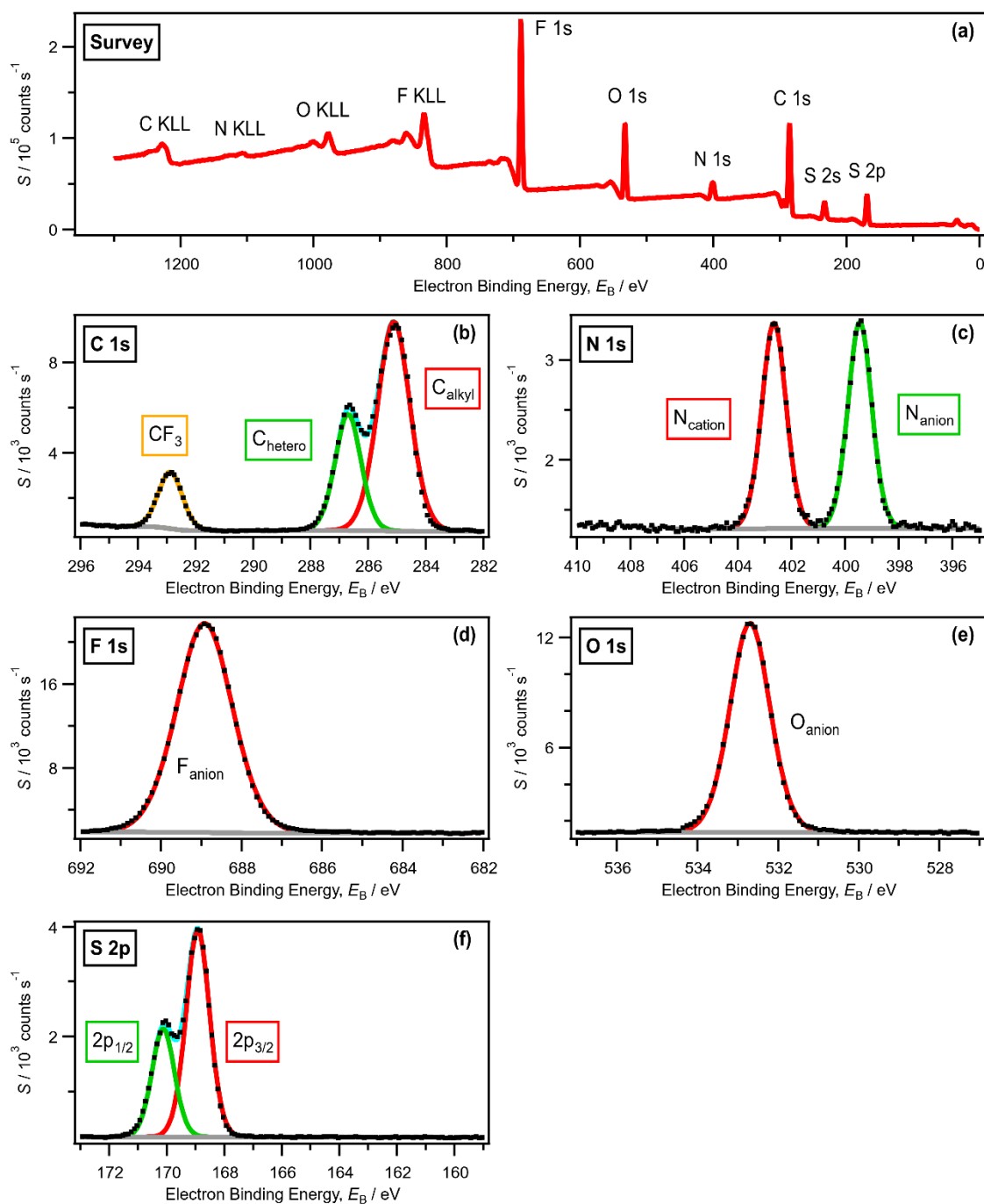


Figure S4. (a) Survey, (b-f) core XP spectra for $[C_8C_1Pyrr][NTf_2]$ recorded on laboratory-based XPS apparatus at $h\nu = 1486.6$ eV. All XP spectra were charge referenced using the method outlined in ESI Section 5.

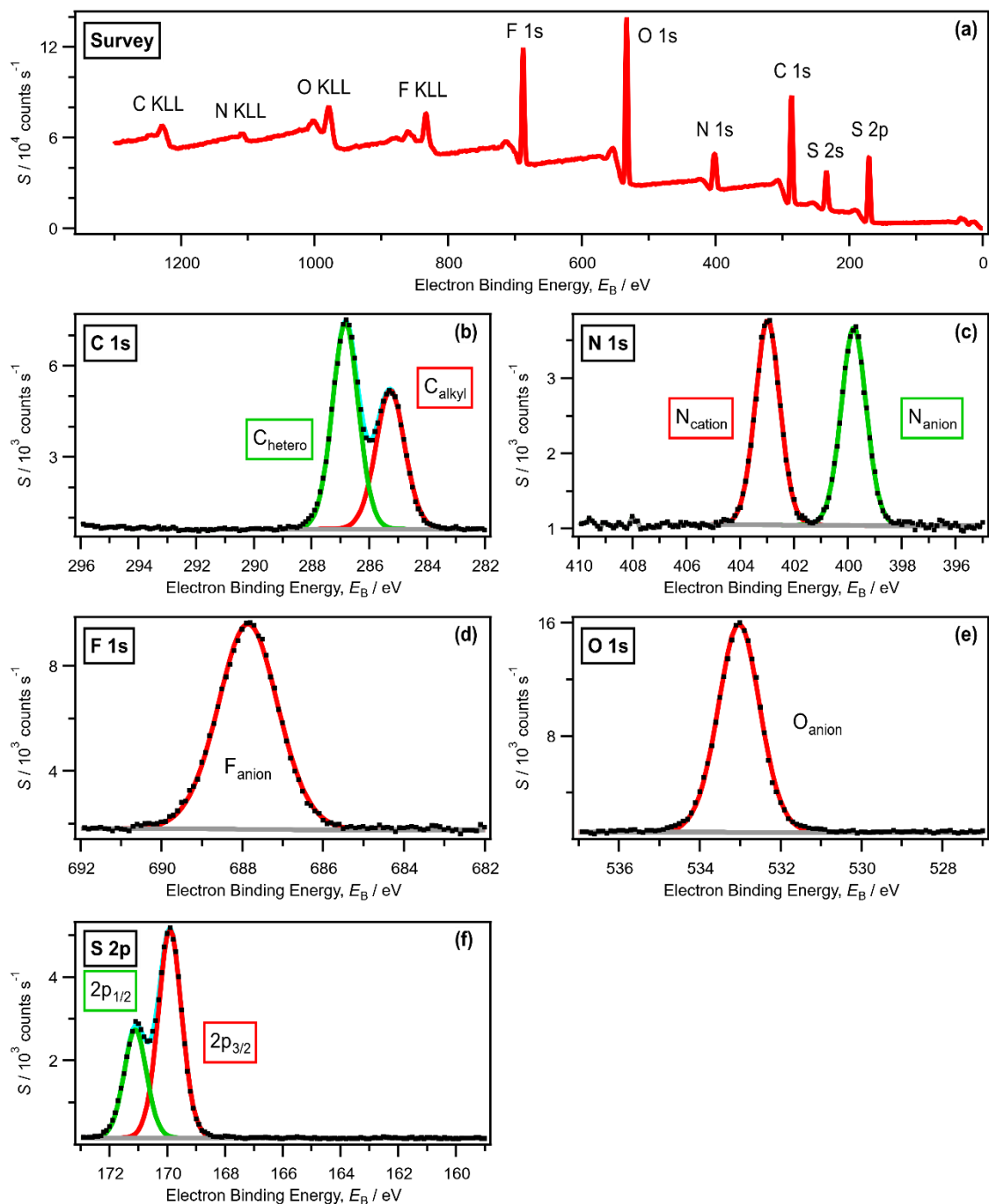


Figure S5. (a) Survey, (b–f) core XP spectra for $[N_{4,1,1,1}][FSI]$ recorded on laboratory-based XPS apparatus at $h\nu = 1486.6 \text{ eV}$. All XP spectra were charge referenced using the method outlined in ESI Section 5.

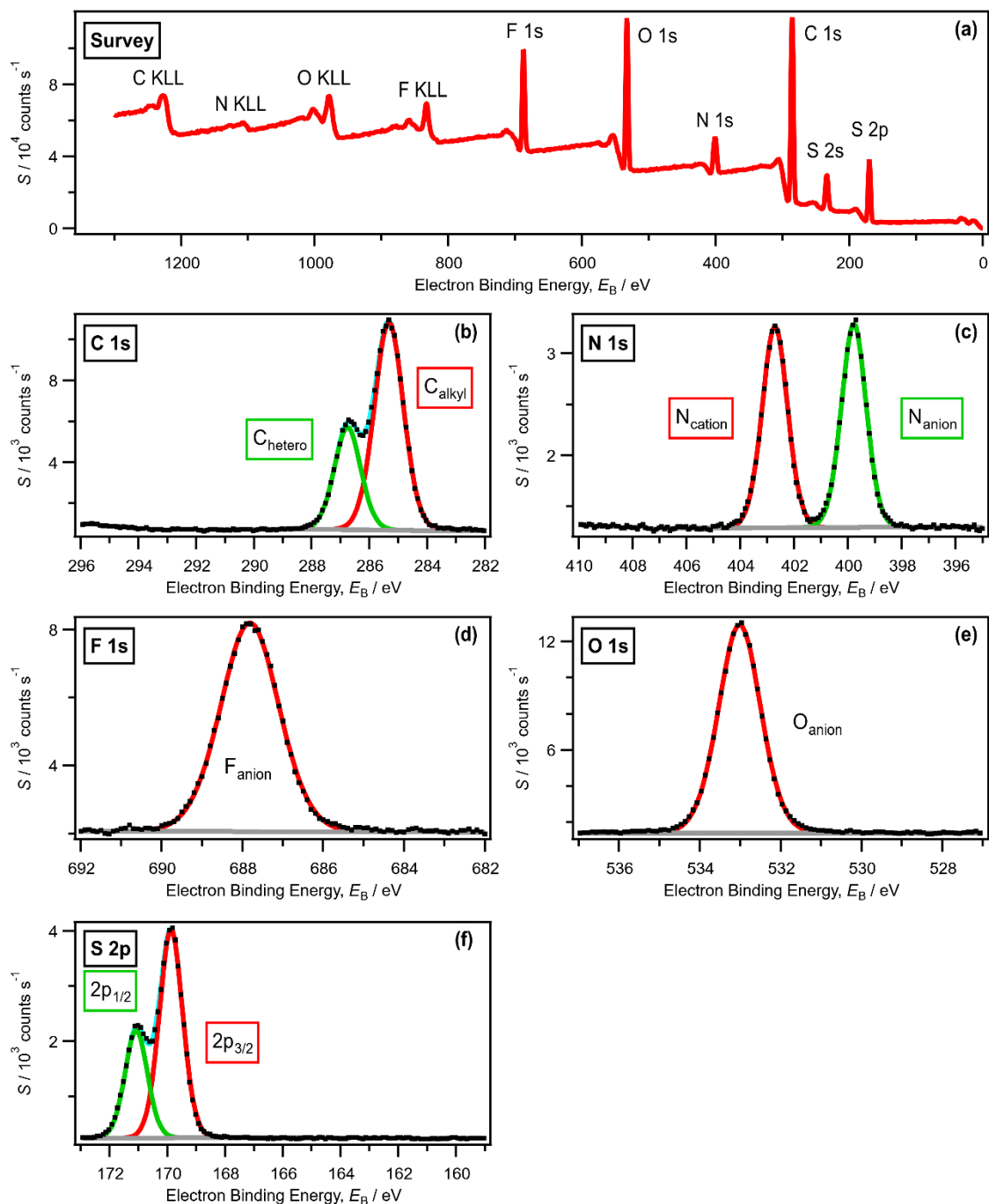


Figure S6. (a) Survey, (b-f) core XP spectra for $[N_{4,4,4,1}][FSI]$ recorded on laboratory-based XPS apparatus at $h\nu = 1486.6 \text{ eV}$. All XP spectra were charge referenced using the method outlined in ESI Section 5.

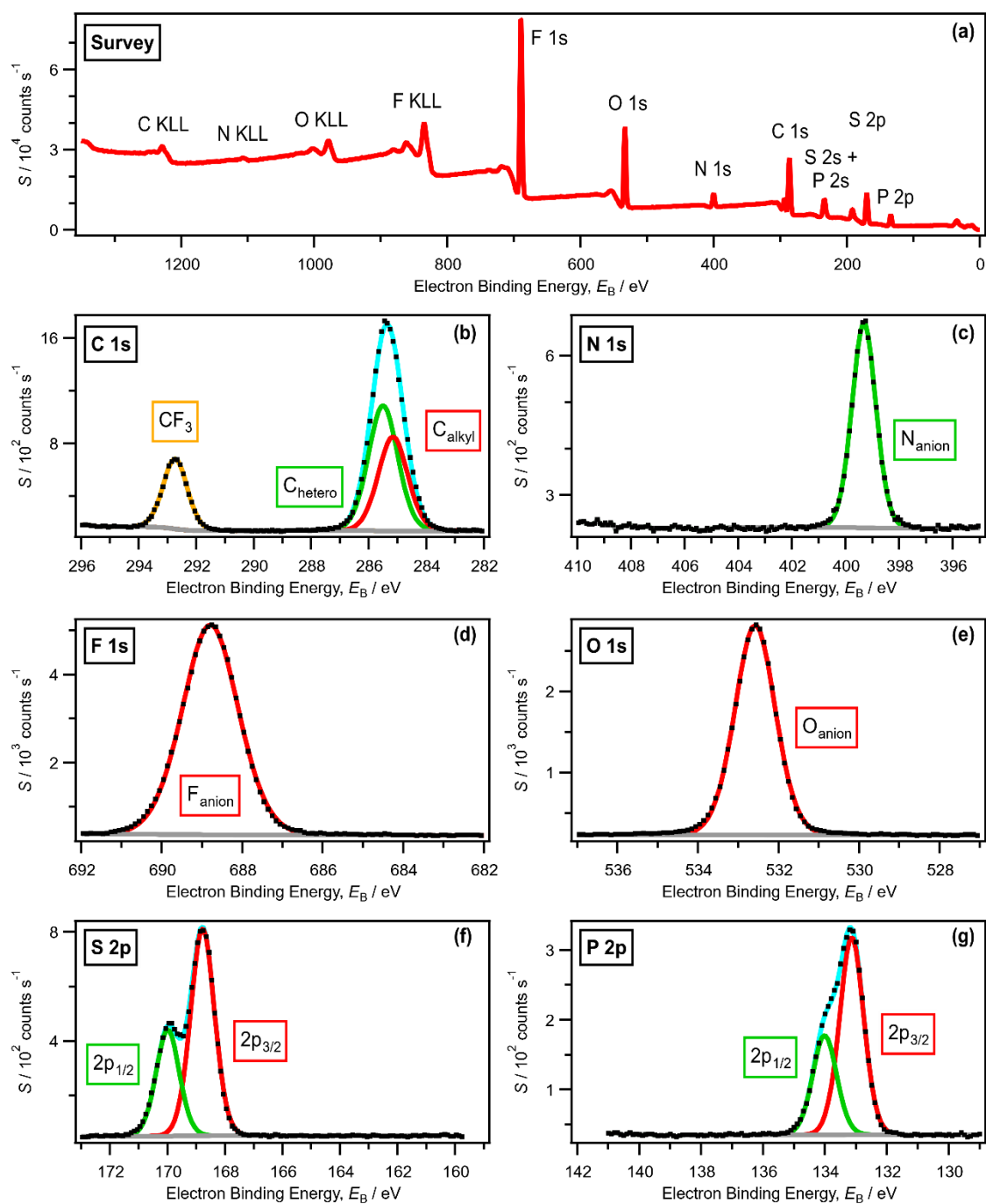


Figure S7. (a) Survey, (b-g) core XP spectra for $[P_{4,1,1,1}][INTf_2]$ recorded on synchrotron-based XPS apparatus at $h\nu = 1486.6$ eV. All XP spectra were charge referenced using the method outlined in ESI Section 5.

6.2. Results. XPS: demonstrating purity using synchrotron-based XPS

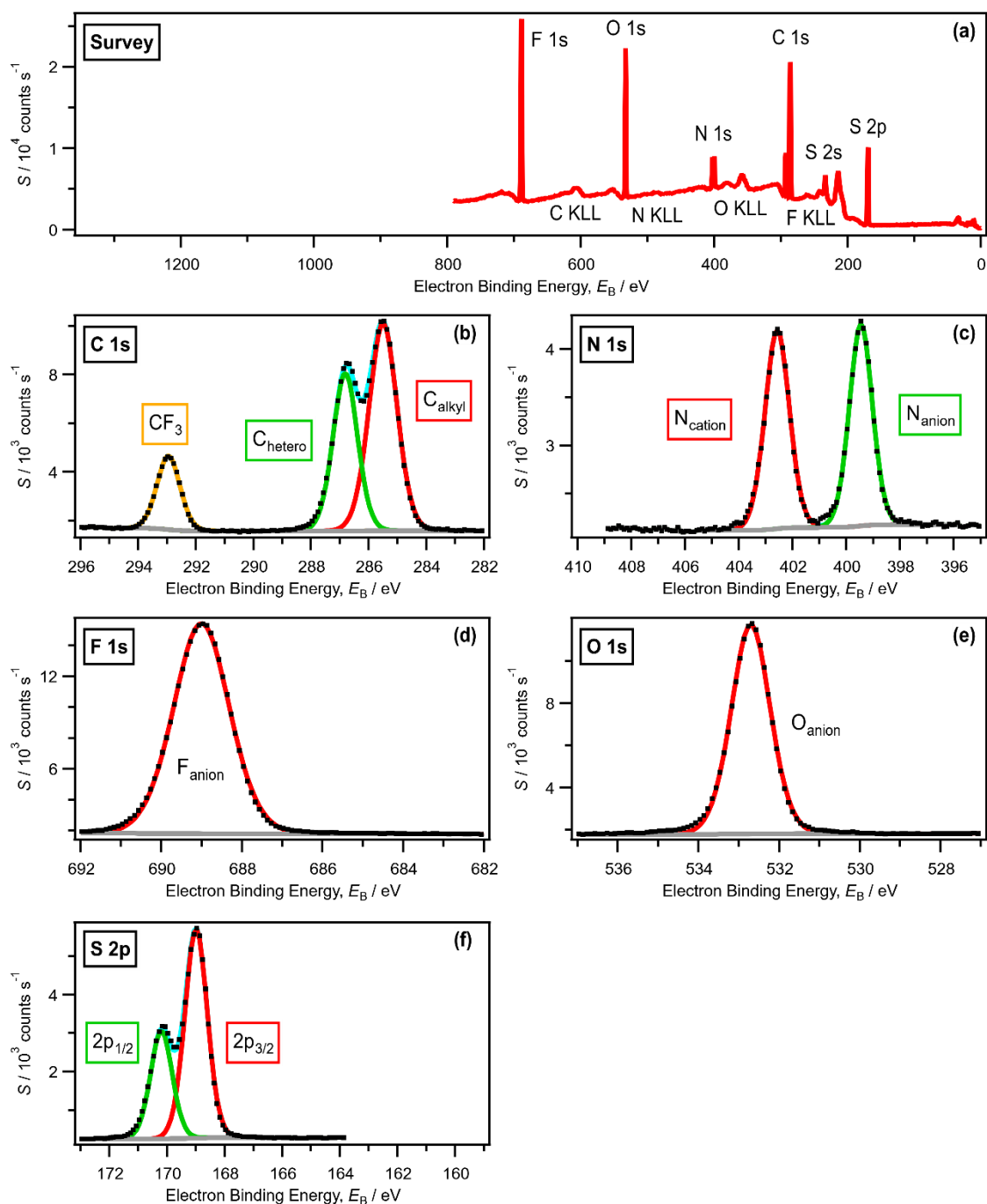


Figure S8 (a) Survey, (b-f) core XP spectra for $[N_{4,2,2,2}][NTf_2]$ recorded on synchrotron-based XPS apparatus at $h\nu = 875$ eV. All XP spectra were charge referenced using the method outlined in ESI Section 5.

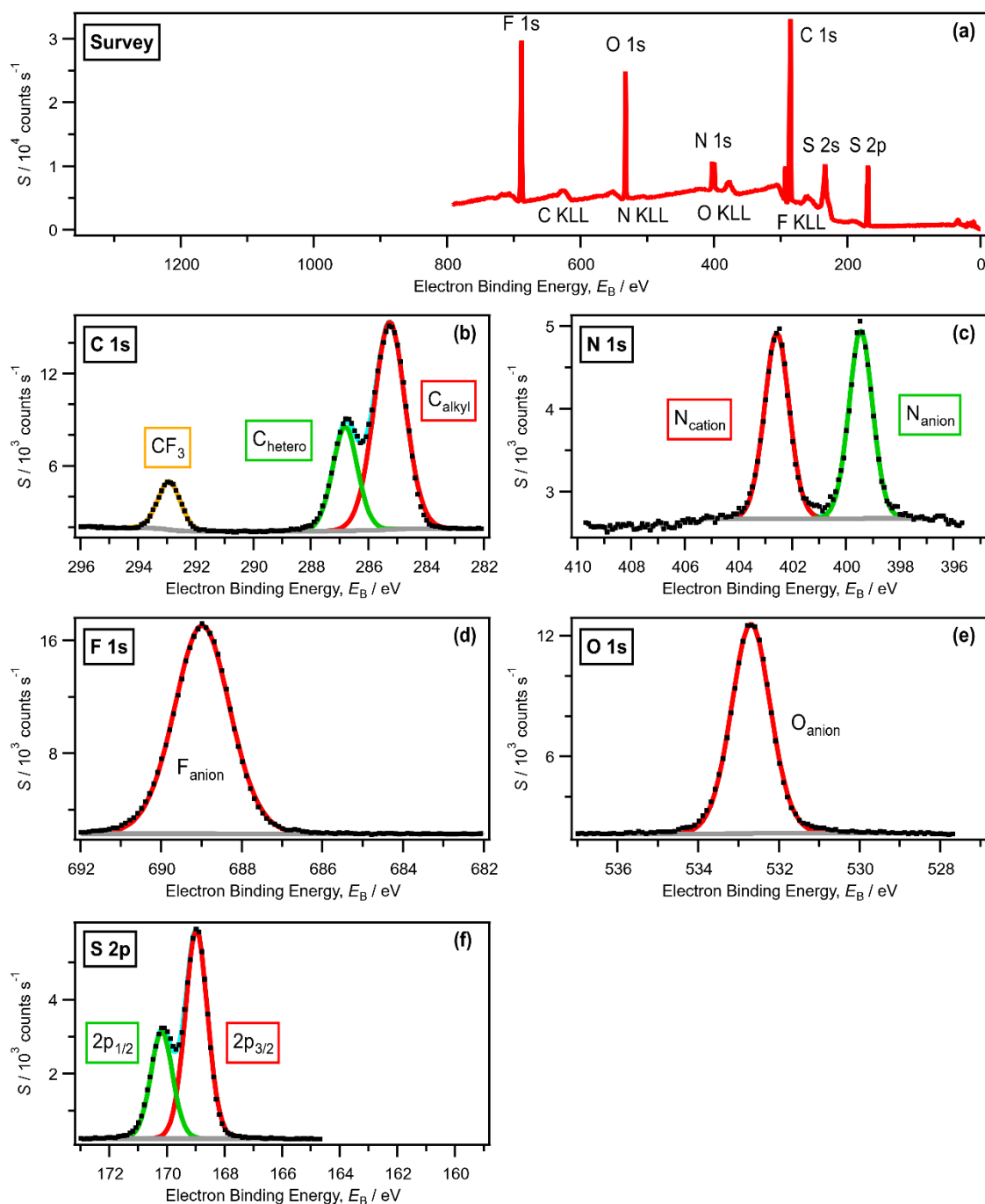


Figure S9. (a) Survey, (b-f) core XP spectra for $[N_{8,2,2,2}][NTf_2]$ recorded on synchrotron-based XPS apparatus at $h\nu = 895 \text{ eV}$. All XP spectra were charge referenced using the method outlined in ESI Section 5.

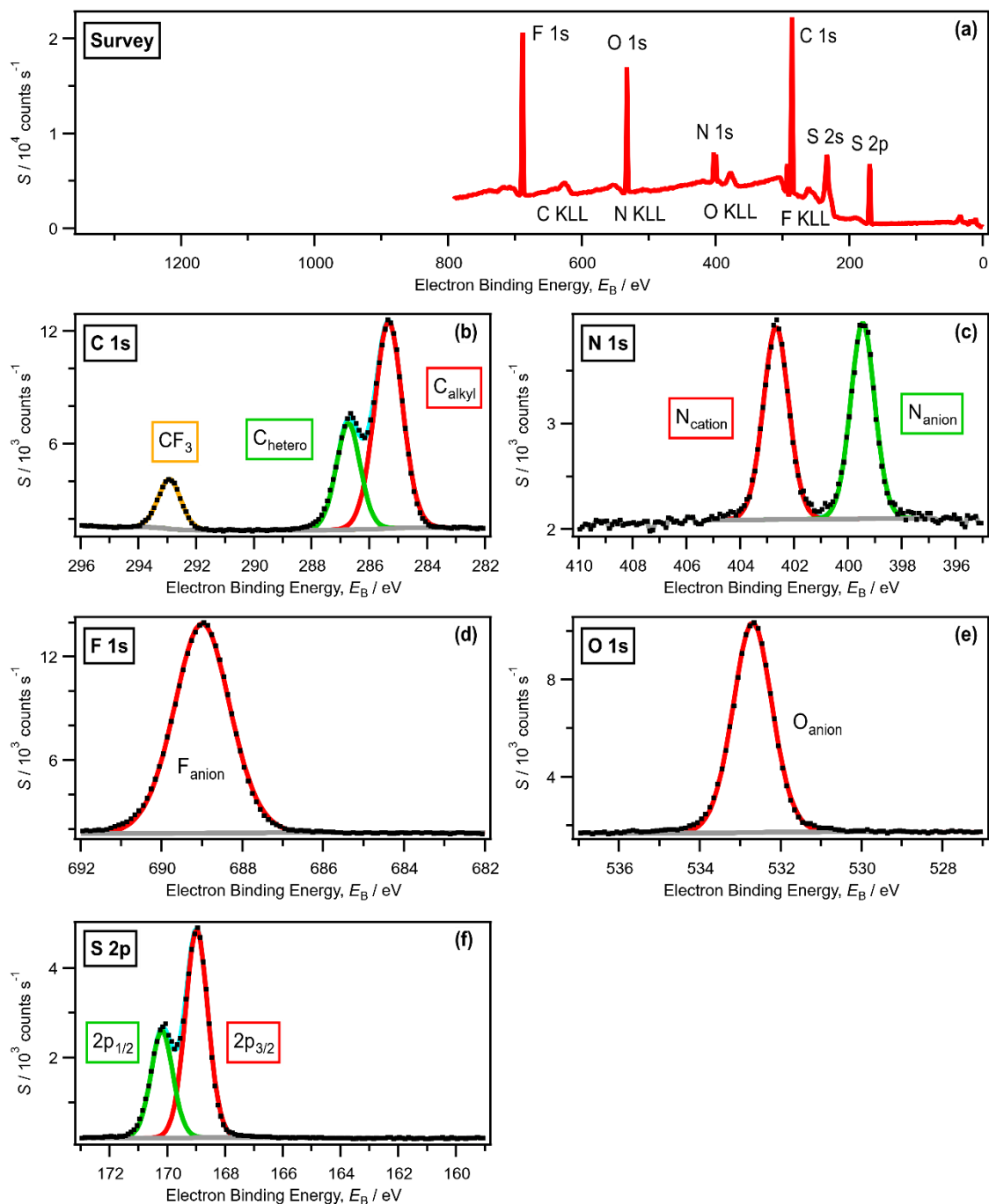


Figure S10. (a) Survey, (b-f) core XP spectra for $[N_{4,4,4,1}][NTf_2]$ recorded on synchrotron-based XPS apparatus at $h\nu = 895 \text{ eV}$. All XP spectra were charge referenced using the method outlined in ESI Section 5.

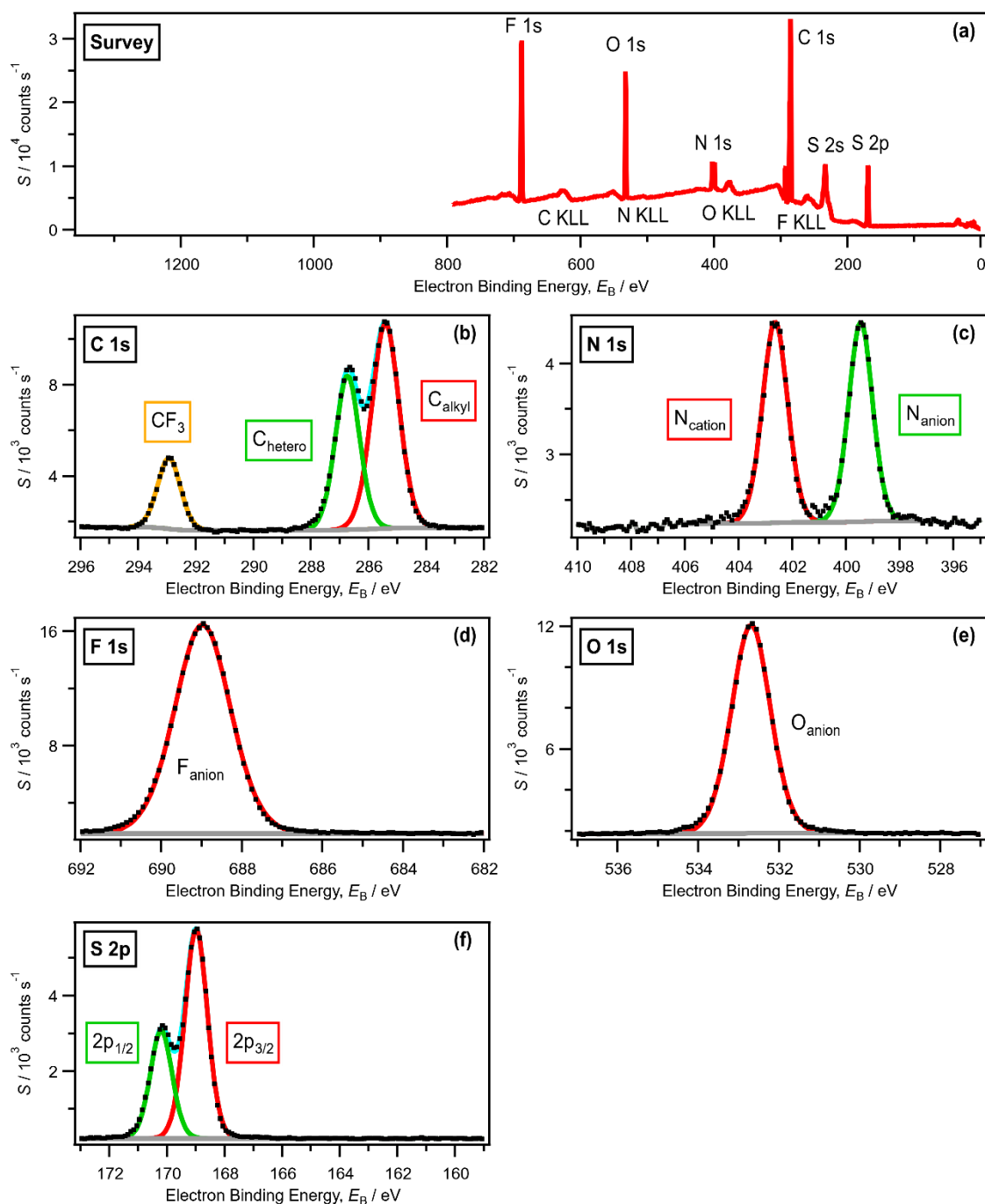


Figure S11. (a) Survey, (b-f) core XP spectra for $[C_4C_1Pip][NTf_2]$ recorded on synchrotron-based XPS apparatus at $h\nu = 895$ eV. All XP spectra were charge referenced using the method outlined in ESI Section 5.

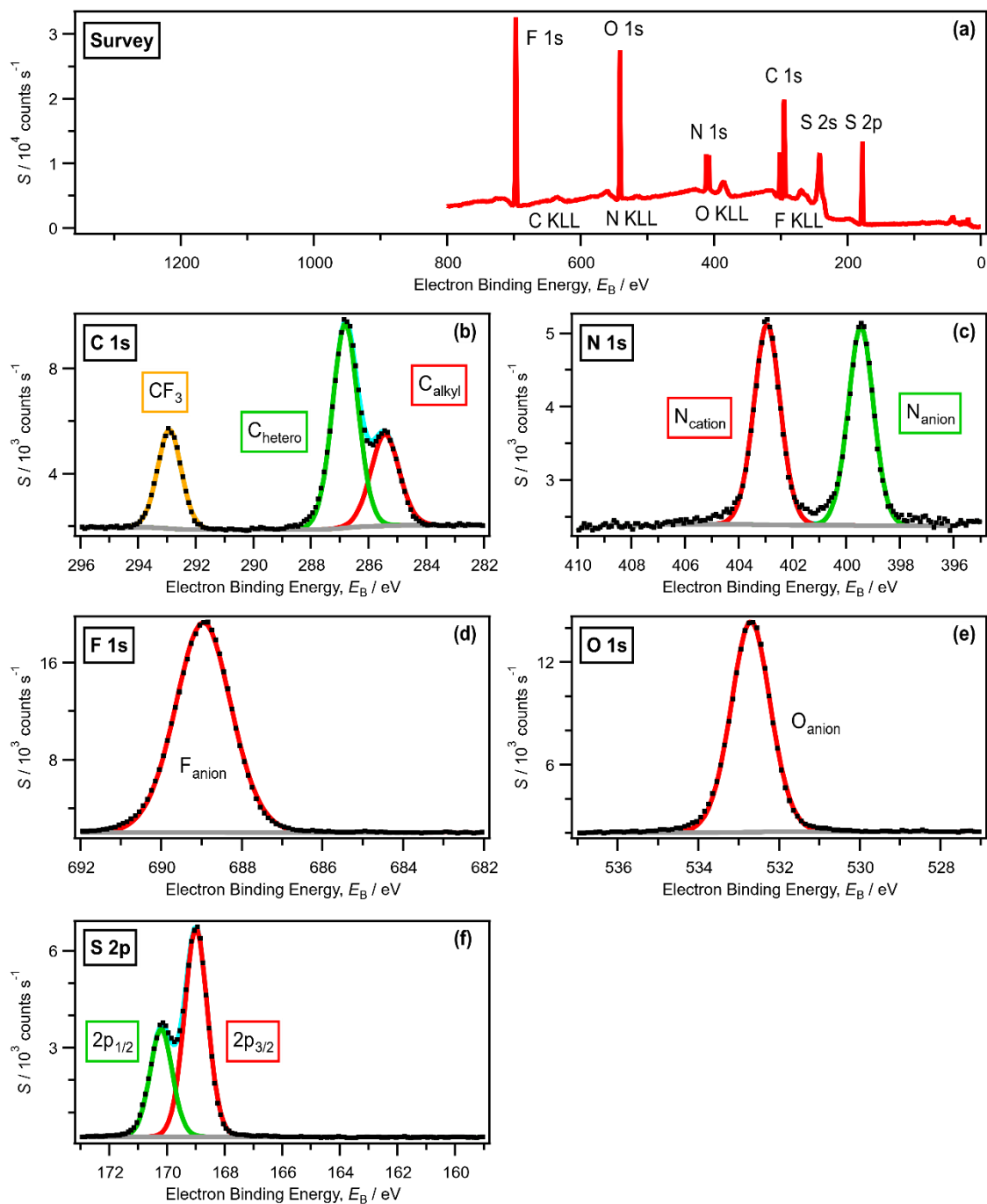


Figure S12. (a) Survey, (b-f) core XP spectra for $[N_{3,1,1,1}][NTf_2]$ recorded on synchrotron-based XPS apparatus at $h\nu = 895$ eV. All XP spectra were charge referenced using the method outlined in ESI Section 5.

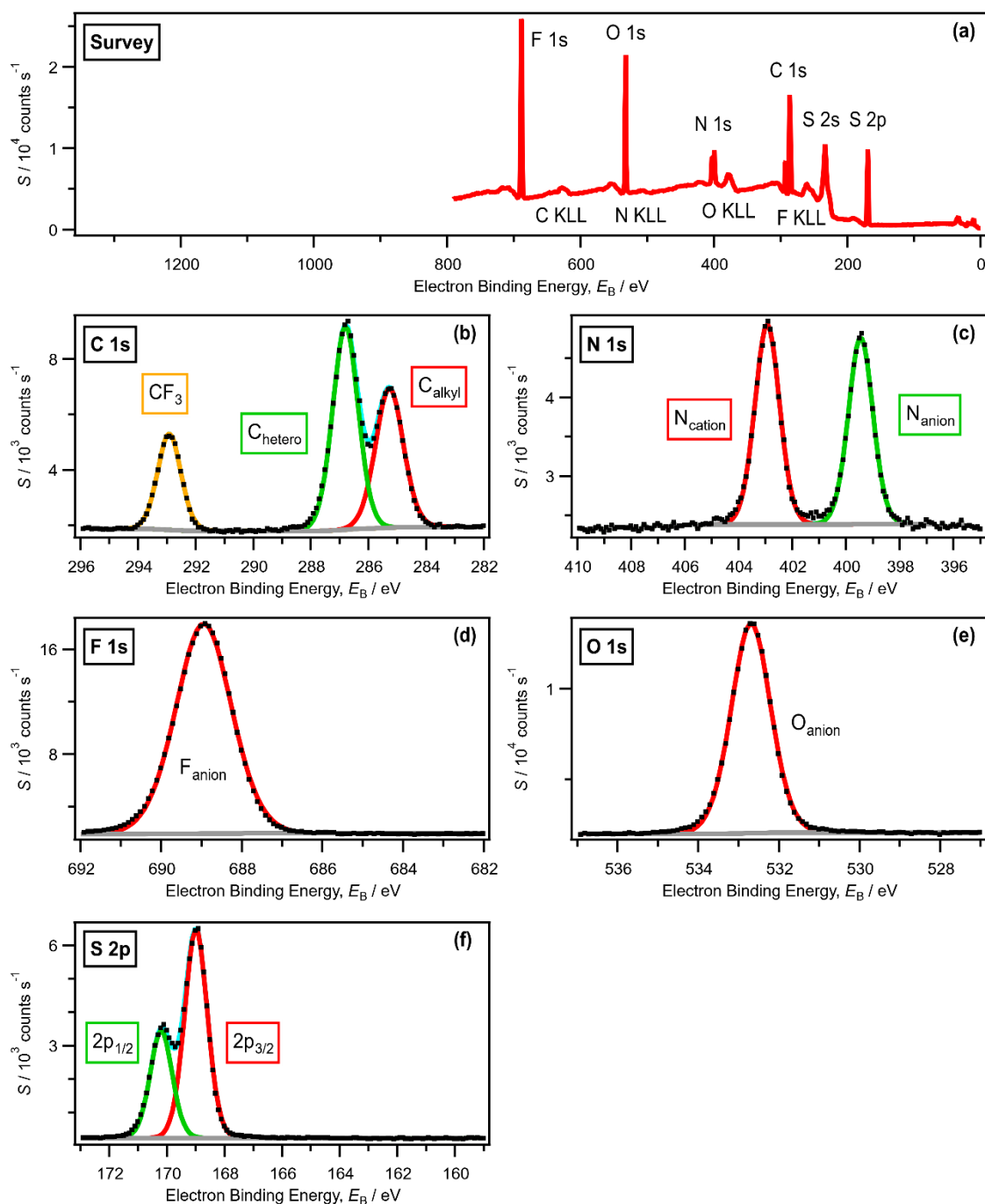


Figure S13. (a) Survey, (b-f) core XP spectra for $[N_{4,1,1,1}][NTf_2]$ recorded on synchrotron-based XPS apparatus at $h\nu = 895$ eV. All XP spectra were charge referenced using the method outlined in ESI Section 5.

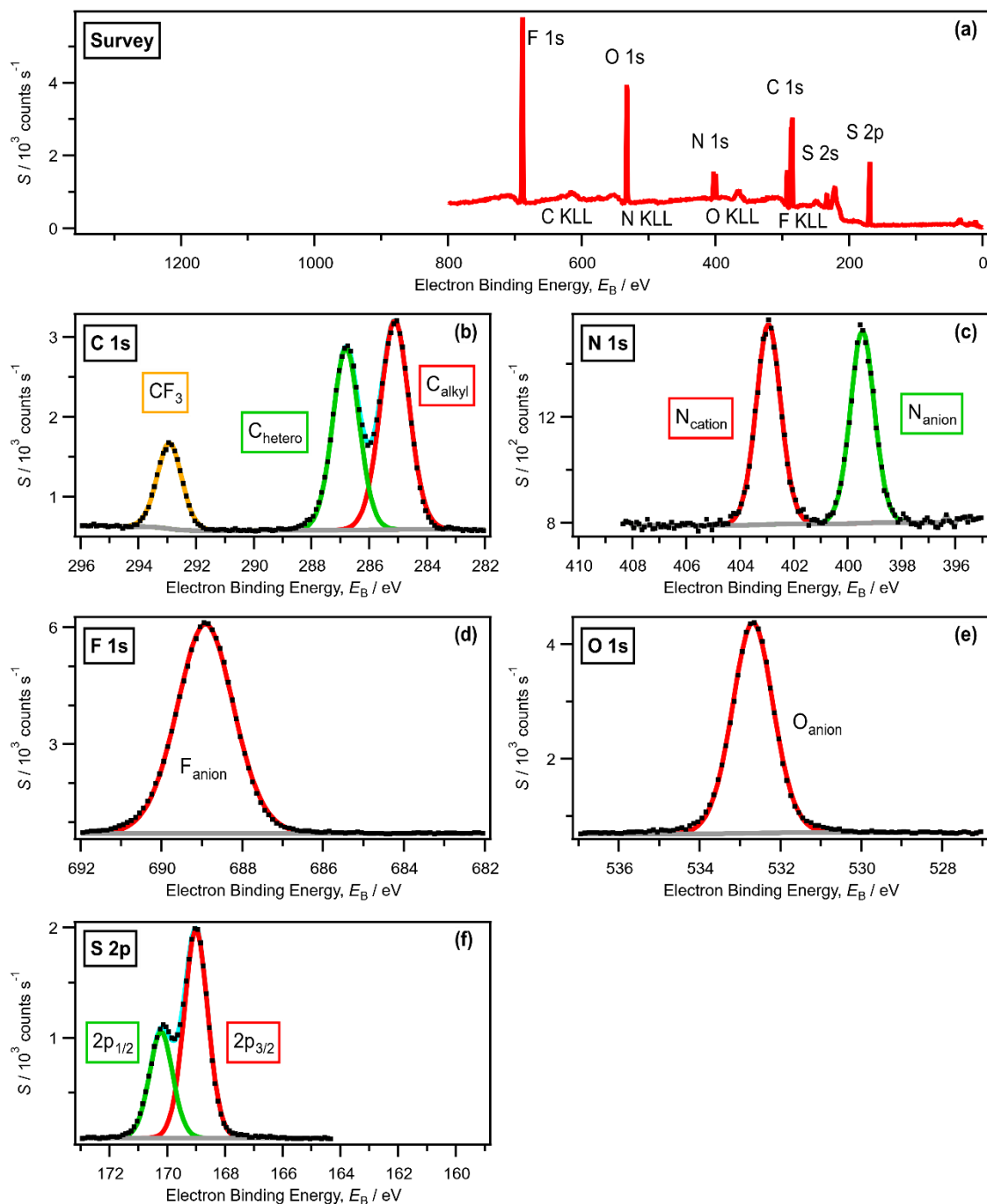


Figure S14. (a) Survey, (b-f) core XP spectra for $[N_{6,1,1,1}][NTf_2]$ recorded on synchrotron-based XPS apparatus at $h\nu = 875 \text{ eV}$. All XP spectra were charge referenced using the method outlined in ESI Section 5.

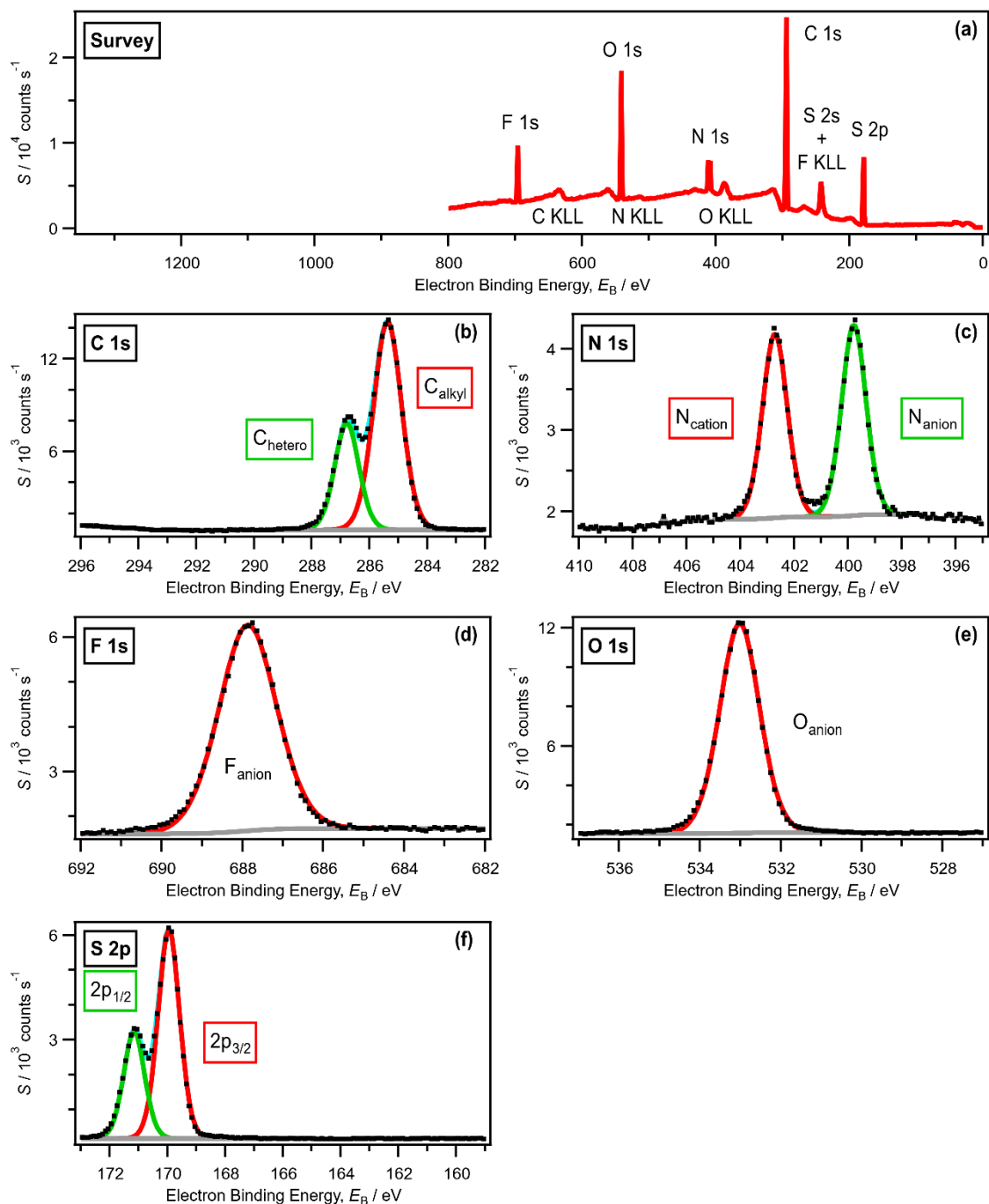


Figure S15. (a) Survey, (b-f) core XP spectra for $[N_{4,4,4,1}][FSI]$ recorded on synchrotron-based XPS apparatus at $h\nu = 895 \text{ eV}$. All XP spectra were charge referenced using the method outlined in ESI Section 5.

The measured experimental and nominal stoichiometries (ESI Table S6) match well for all four ILs newly investigated here using lab XPS. Differences, especially the larger carbon values relative to other elements, are likely due to differences in relative sensitivity factors (RSF) values, as these RSF values were not tuned specially to the Reading and UCL XPS apparatus (in references ^{3, 19} RSF values were tuned specially to the XPS apparatus used in those studies).

The measured experimental and nominal stoichiometries (ESI Table S7) match well for all eight ILs investigated here using synchrotron XPS. Excellent visual matches for N 1s and C 1s XP spectra were found when the same IL was measured on different apparatus (ESI Figure S16). All these matches, along with the high quality XP spectra given in ESI Figure S2 to ESI Figure S15, demonstrates the high purity of the IL samples newly presented here.

Table S6. Measured experimental and nominal (in brackets) stoichiometries for the ionic liquids studied in this work, recorded at $h\nu = 1486.6$ eV.

IL no.	Abbreviation	RSF ^a	F 1s	O 1s	N 1s	C 1s	S 2p _{3/2}	P 2p _{3/2}
			1.000	0.580	0.350	0.205	0.267	0.200
	[N _{4,2,2,2}][NTf ₂]	Measured (nominal)		3.7 (4)	2.0 (2)	12.2 (12)	2.1 (2)	
	[C ₈ C ₁ Pyrr][NTf ₂]	Measured (nominal)	5.2 (6)	3.7 (4)	2.0 (2)	15.8 (15)	2.2 (2)	
	[N _{4,1,1,1}][FSI]	Measured (nominal)	1.7 (2)	3.7 (4)	2.0 (2)	7.4 (7)	2.2 (2)	
	[N _{4,4,4,1}][FSI]	Measured (nominal)	1.7 (2)	3.9 (4)	2.0 (2)	13.4 (13)	2.1 (2)	
	[P _{i4,1,1,1}][NTf ₂]	Measured (nominal)	5.8 (6)	3.9 (4)	1.0 (1)	9.2 (9)	2.1 (2)	1.0 (1)

^a RSF = relative sensitivity factors, taken from reference ¹⁹ for C 1s, N 1s, O 1s, F 1s, S 2p_{3/2}, P 2p_{3/2}

Table S7. Measured experimental and nominal (in brackets) stoichiometries for the ionic liquids studied in this work, recorded at either $h\nu = 875$ eV or $h\nu = 895$ eV.

IL no.	Abbreviation	RSF ^a	F 1s	O 1s	N 1s	C 1s	S 2p _{3/2}
			1.000	0.800	0.600	0.410	0.700
	[N _{4,2,2,2}][NTf ₂]	Measured (nominal)	5.9 (6)	3.8 (4)	1.9 (2)	12.5 (12)	1.9 (2)
	[N _{8,2,2,2}][NTf ₂]	Measured (nominal)	6.0 (6)	3.7 (4)	2.0 (2)	16.5 (16)	1.8 (2)
	[N _{4,4,4,1}][NTf ₂]	Measured (nominal)	6.0 (6)	3.8 (4)	2.0 (2)	15.3 (15)	1.9 (2)
	[C ₄ C ₁ Pip][NTf ₂]	Measured (nominal)	6.1 (6)	3.7 (4)	2.0 (2)	12.3 (12)	1.9 (2)
	[N _{3,1,1,1}][NTf ₂]	Measured (nominal)	6.0 (6)	3.8 (4)	2.2 (2)	8.2 (8)	1.8 (2)
	[N _{4,1,1,1}][NTf ₂]	Measured (nominal)	6.0 (6)	3.8 (4)	2.0 (2)	9.3 (9)	1.9 (2)
	[N _{6,1,1,1}][NTf ₂]	Measured (nominal)	6.2 (6)	3.8 (4)	1.8 (2)	11.3 (11)	1.8 (2)
	[N _{4,4,4,1}][FSI]	Measured (nominal)	1.9 (2)	3.8 (4)	2.1 (2)	13.4 (13)	1.9 (2)

^a RSF = relative sensitivity factors adapted based on data and known stoichiometry for C 1s, N 1s, O 1s, F 1s, S 2p_{3/2}

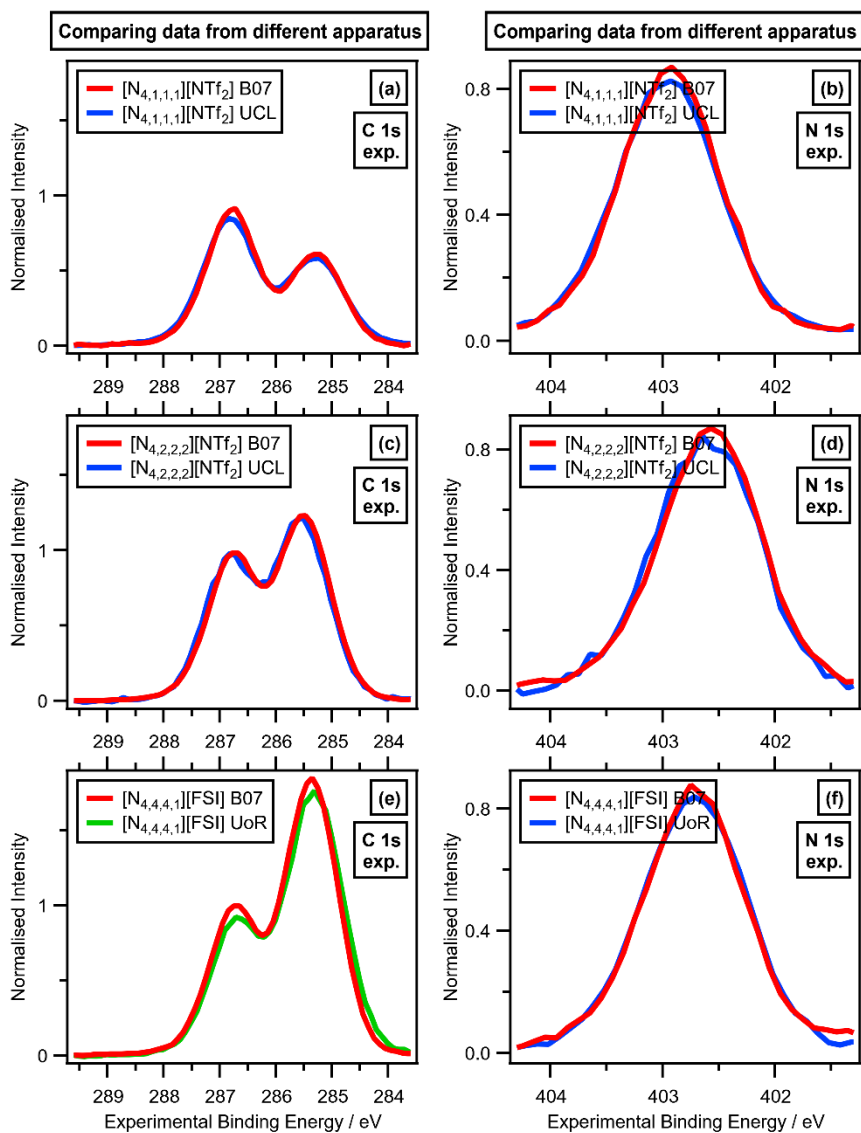


Figure S16. Comparison for the same ionic liquids measured on different XPS apparatus. $[N_{4,1,1,1}][NTf_2]$ on B07 and UCL: (a) C 1s, (b) N 1s. $[N_{4,2,2,2}][NTf_2]$ on B07 and UCL: (c) C 1s, (d) N 1s. $[N_{4,4,4,1}][FSI]$ on B07 and UoR: (e) C 1s, (f) N 1s. Experimental XP spectra are area normalised and charge referenced using methods given in ESI Section 5.

7. Results. Experimental and calculated $E_B(\text{X core})$

Table S8. Experimental $E_B(\text{N}_{\text{cation}} 1s)$ and $E_B(\text{S}_{\text{cation}} 2p_{3/2})$ for ILs investigated using X-ray photoelectron spectroscopy (XPS) in this work

IL no.	Abbreviation	Where measured	$E_B(\text{N}_{\text{cation}} 1s, \text{exp})$ / eV	Average $E_B(\text{N}_{\text{cation}} 1s, \text{exp})$ / eV	$E_B(\text{S}_{\text{cation}} 2p_{3/2}, \text{exp})$ / eV
1	$[\text{N}_{4,2,2,2}][\text{NTf}_2]$	B07	402.61		
1	$[\text{N}_{4,2,2,2}][\text{NTf}_2]$	UCL (Theta Probe)	402.64	402.63	
2	$[\text{N}_{8,2,2,2}][\text{NTf}_2]$	B07	402.62		
3	$[\text{N}_{4,4,4,1}][\text{NTf}_2]$	B07	402.72		
4	$[\text{N}_{8,8,8,1}][\text{NTf}_2]$	UoR	402.73		
5	$[\text{C}_4\text{C}_1\text{Pip}][\text{NTf}_2]$	B07	402.68	402.71	
6	$[\text{C}_8\text{C}_1\text{Pyrr}][\text{NTf}_2]$	UoR	402.70		
7	$[\text{N}_{3,2,1,1}][\text{NTf}_2]$	UCL ($\text{K}\alpha$)	402.85	N/A	
8	$[\text{N}_{3,1,1,1}][\text{NTf}_2]$	B07	402.99		
9	$[\text{N}_{4,1,1,1}][\text{NTf}_2]$	B07	402.98		
9	$[\text{N}_{4,1,1,1}][\text{NTf}_2]$	UCL ($\text{K}\alpha$)	403.00	402.99	
10	$[\text{N}_{6,1,1,1}][\text{NTf}_2]$	B07	402.99		
11	$[\text{N}_{4,1,1,1}][\text{FSI}]$	UoR	402.99	N/A	
12	$[\text{N}_{4,4,4,1}][\text{FSI}]$	UoR	402.72		
12	$[\text{N}_{4,4,4,1}][\text{FSI}]$	B07	402.72	402.72	
13	$[\text{S}_{2,2,1}][\text{NTf}_2]$	UCL ($\text{K}\alpha$)	N/A	N/A	166.51
14	$[\text{S}_{2,2,2}][\text{NTf}_2]$	UCL ($\text{K}\alpha$)	N/A	N/A	166.35

Table S9. $E_B(N_{\text{cation}} 1s)$ for onium cations investigated using calculations in this work

Cation no.	Abbreviation	$E_B(N_{\text{cation}} 1s, \text{calc})$ using IL SMD / eV	$E_B(N_{\text{cation}} 1s, \text{calc})$ using water SMD / eV	$E_B(N_{\text{cation}} 1s, \text{calc})$ in GP / eV
1	$[N_{i3,i3,i3,i3}]^+$	396.29		
2	$[N_{2,2,2,2}]^+$	396.38	396.05	400.44
3	$[N_{4,2,2,2}]^+$	396.39		400.34
4	$[N_{8,2,2,2}]^+$	396.38		400.29
5	$[N_{2,2,2,1}]^+$	396.45	396.11	400.64
6	$[N_{4,4,4,1}]^+$	396.48		
7	$[C_4C_1\text{Pip}]^+$	396.46		
8	$[C_4C_1\text{Pyrr}]^+$	396.40		
9	$[C_8C_1\text{Pyrr}]^+$	396.39		
10	$[N_{3,2,1,1}]^+$	396.55		
11	$[N_{2,2,1,1}]^+$	396.54	396.18	400.87
12	$[N_{2,1,1,1}]^+$	396.63	396.26	401.11
13	$[N_{3,1,1,1}]^+$	396.63		401.03
14	$[N_{4,1,1,1}]^+$	396.63		400.98
15	$[N_{6,1,1,1}]^+$	396.63		400.94
16	$[N_{8,1,1,1}]^+$	396.62		
17	$[N_{16,1,1,1}]^+$	396.62		
18	$[N_{1,1,1,1}]^+$	396.72	396.33	401.37

Table S10. $E_B(S_{\text{cation}} 2p)$ for onium cations investigated using calculations in this work

Cation no.	Abbreviation	$E_B(S_{\text{cation}} 2p, \text{calc})$ using IL SMD / eV	Average $E_B(S_{\text{cation}} 2p, \text{calc})$ using IL SMD / eV	Average $E_B(S_{\text{cation}} 2p_{3/2}, \text{calc})$ using IL SMD / eV
19	[S _{2,2,2}] ⁺	166.11	166.06	165.26
		166.11		
		165.97		
20	[S _{2,2,1}] ⁺	166.22	166.16	165.36
		166.21		
		166.07		
21	[S _{2,1,1}] ⁺	166.36	166.31	165.51
		166.35		
		166.21		
22	[S _{1,1,1}] ⁺	166.48	166.44	165.64
		166.48		
		166.34		

For Figure 3, the cations used were [P_{2,2,2,2}]⁺, [P_{4,4,4,1}]⁺, [P_{3,2,1,1}]⁺, [P_{4,1,1,1}]⁺ and [P_{1,1,1,1}]⁺.

Table S11. $E_B(P_{\text{cation}} 2p)$ for onium cations investigated using calculations in this work

Cation no.	Abbreviation	$E_B(P_{\text{cation}} 2p, \text{calc})$ using IL SMD / eV	Average $E_B(P_{\text{cation}} 2p, \text{calc})$ using IL SMD / eV	Average $E_B(P_{\text{cation}} 2p_{3/2}, \text{calc})$ using IL SMD / eV
23	[P _{2,2,2,2}] ⁺	132.74	132.74	132.16
		132.74		
		132.74		
24	[P _{4,2,2,2}] ⁺	132.74	132.74	132.16
		132.73		
		132.74		
25	[P _{8,2,2,2}] ⁺	132.74	132.74	132.16
		132.74		
		132.81		
26	[P _{4,4,4,1}] ⁺	132.81	132.81	132.23
		132.80		
		132.78		
27	[C ₄ C ₁ phin] ⁺	132.78	132.78	132.20
		132.78		
		132.82		
28	[C ₄ C ₁ phol] ⁺	132.82	132.82	132.24
		132.81		
		132.87		
29	[P _{3,2,1,1}] ⁺	132.87	132.87	132.29
		132.86		
		132.94		
30	[P _{4,1,1,1}] ⁺	132.94	132.94	132.36
		132.94		
		133.01		
31	[P _{1,1,1,1}] ⁺	133.01	133.01	132.43
		133.01		

8. Results. Experimental N 1s XP spectra: effect of [FSI]⁻ versus [NTf₂]⁻

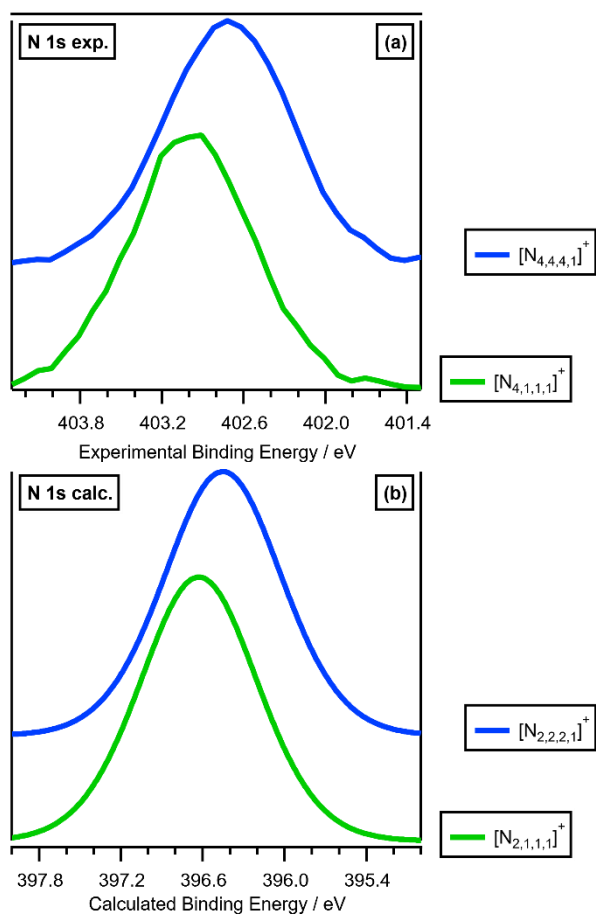


Figure S17. Demonstrating that the effect of the alkyl chain lengths on cation electronic structure is independent of the anion identity. XPS for N 1s [N_{4,4,4,1}]⁺[FSI]⁻ versus [N_{4,1,1,1}]⁺[FSI]⁻: (a) experimental, (b) calculated.

9. Results. Experimental versus calculated N 1s XP spectra

The exceptions are the Pyrr-containing cations $[\text{C}_4\text{C}_1\text{Pyrr}]^+$ and $[\text{C}_8\text{C}_1\text{Pyrr}]^+$, which gave slightly smaller $E_{\text{B}}(\text{N}_{\text{cation}}\ 1\text{s})$ than expected (~ 0.06 eV lower than $[\text{N}_{2,2,2,1}]^+$) based on the experimental data and calculations for $[\text{N}_{2,2,2,1}]^+$, $[\text{N}_{4,4,4,1}]^+$ and $[\text{C}_4\text{C}_1\text{Pip}]^+$ (ESI Figure S18). However, this effect is unlikely to be caused by a ring effect, given that the Pip-containing cation $[\text{C}_4\text{C}_1\text{Pip}]^+$ gave calculated $E_{\text{B}}(\text{N}_{\text{cation}}\ 1\text{s})$ as expected based on experimental data (ESI Figure S18).

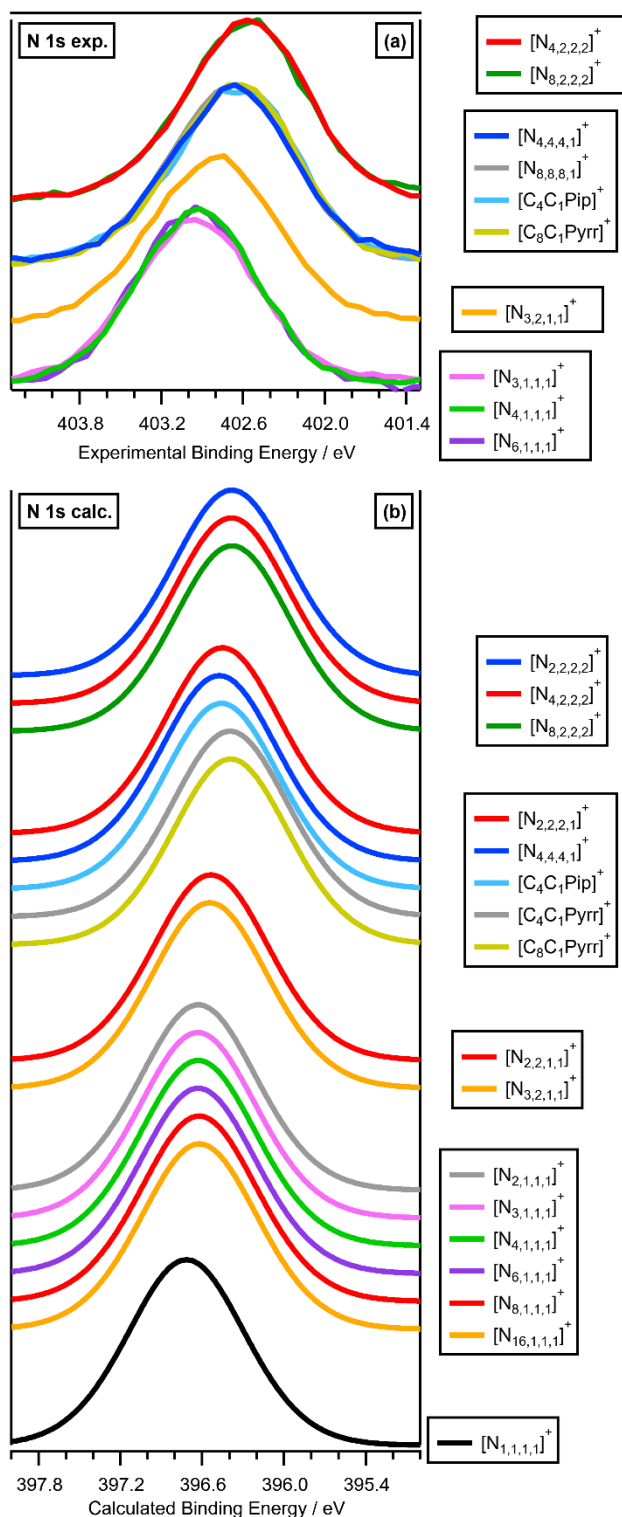


Figure S18. Experimental and calculated core XP spectra: (a) N 1s,exp. for [N_{3,1,1,1}][NTf₂], [N_{4,1,1,1}][NTf₂], [N_{6,1,1,1}][NTf₂], [N_{3,2,1,1}][NTf₂], [N_{4,4,4,1}][NTf₂], [N_{8,8,8,1}][NTf₂], [C₄C₁Pip][NTf₂], [C₈C₁Pyrr][NTf₂], [N_{4,2,2,2}][NTf₂] and [N_{8,2,2,2}][NTf₂]; (b) N 1s,calc. for [N_{1,1,1,1}]⁺, [N_{2,1,1,1}]⁺, [N_{3,1,1,1}]⁺, [N_{4,1,1,1}]⁺, [N_{6,1,1,1}]⁺, [N_{8,1,1,1}]⁺, [N_{16,1,1,1}]⁺, [N_{2,2,1,1}]⁺, [N_{3,2,1,1}]⁺, [N_{2,2,2,1}]⁺, [N_{4,4,4,1}]⁺, [C₄C₁Pip]⁺, [C₄C₁Pyrr]⁺, [C₈C₁Pyrr]⁺, [N_{2,2,2,2}]⁺, [N_{4,2,2,2}]⁺, and [N_{8,2,2,2}]⁺. Experimental XP spectra are area normalised and charge referenced using methods given in ESI Section 5. Traces are vertically offset for clarity.

10. Results. Effect of SMD parameters/gas-phase on N 1s XP spectra

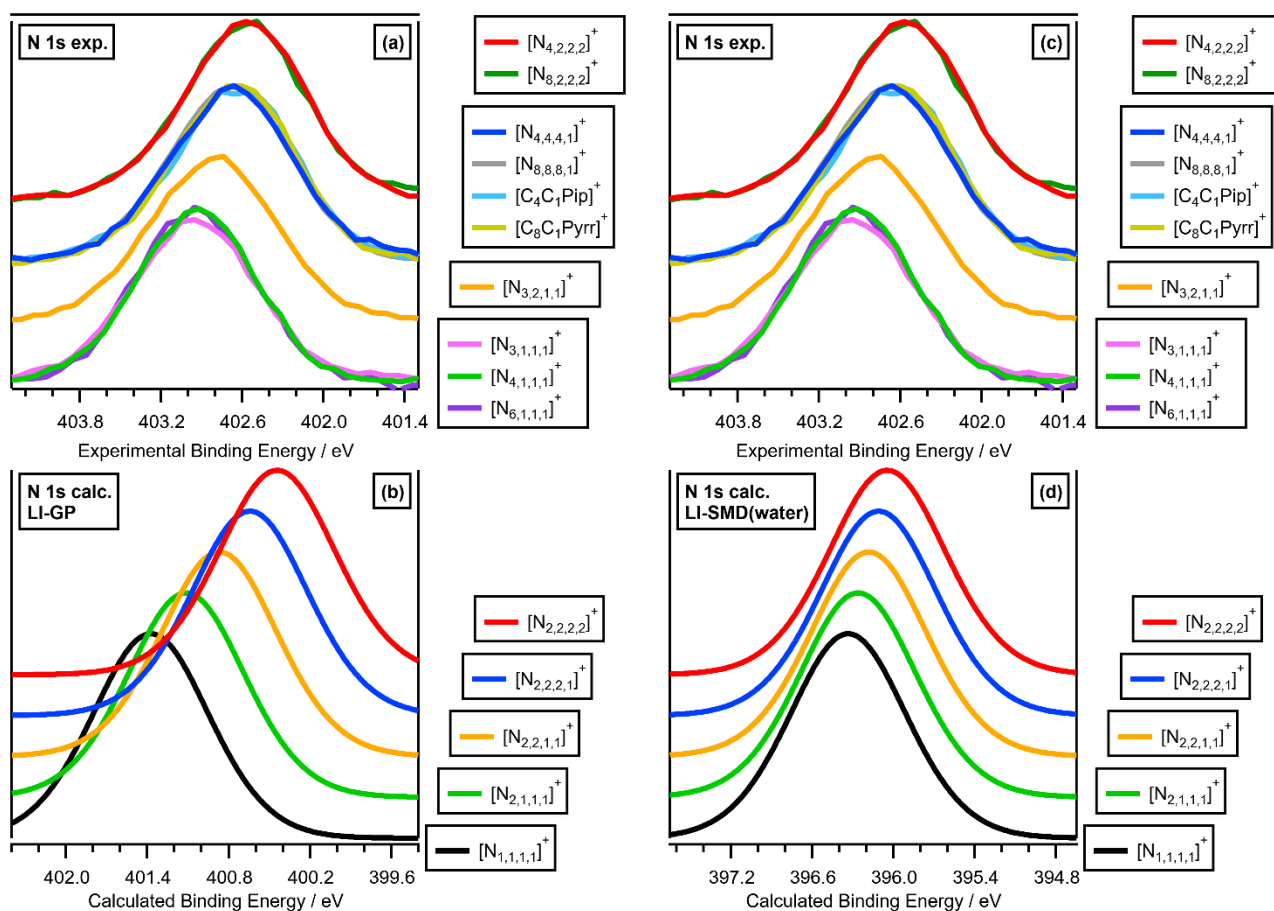


Figure S19. N 1s XP spectra. (a) and (c) Experimental N 1s XP spectra N 1s,exp., for: $[N_{3,1,1,1}][NTf_2]$, $[N_{4,1,1,1}][NTf_2]$, $[N_{6,1,1,1}][NTf_2]$, $[N_{3,2,1,1}][NTf_2]$, $[N_{4,4,4,1}][NTf_2]$, $[N_{8,8,8,1}][NTf_2]$, $[C_4C_1Pip][NTf_2]$, $[C_8C_1Pyrr][NTf_2]$, $[N_{4,2,2,2}][NTf_2]$ and $[N_{8,2,2,2}][NTf_2]$. Calculated N 1s XP spectra, N 1s,calc., for $[N_{1,1,1,1}]^+$, $[N_{2,1,1,1}]^+$, $[N_{2,2,1,1}]^+$, $[N_{2,2,2,1}]^+$ and $[N_{2,2,2,2}]^+$: (b) gas phase, (d) water SMD. Experimental XP spectra are area normalised and charge referenced using methods given in ESI Section 5. Traces are vertically offset for clarity.

11. Results. Linear correlations of calculated versus experimental $E_B(N_{\text{cation}} 1s)$

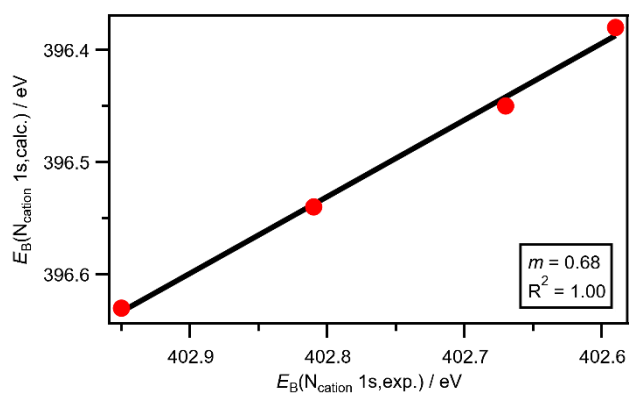


Figure S20. Calculated versus experimental $E_B(N_{\text{cation}} 1s)$. Calculated data for the cations $[\text{N}_{2,1,1,1}]^+$, $[\text{N}_{2,2,1,1}]^+$, $[\text{N}_{2,2,2,1}]^+$ and $[\text{N}_{2,2,2,2}]^+$.

12. Results. Calculated P 2p XPS

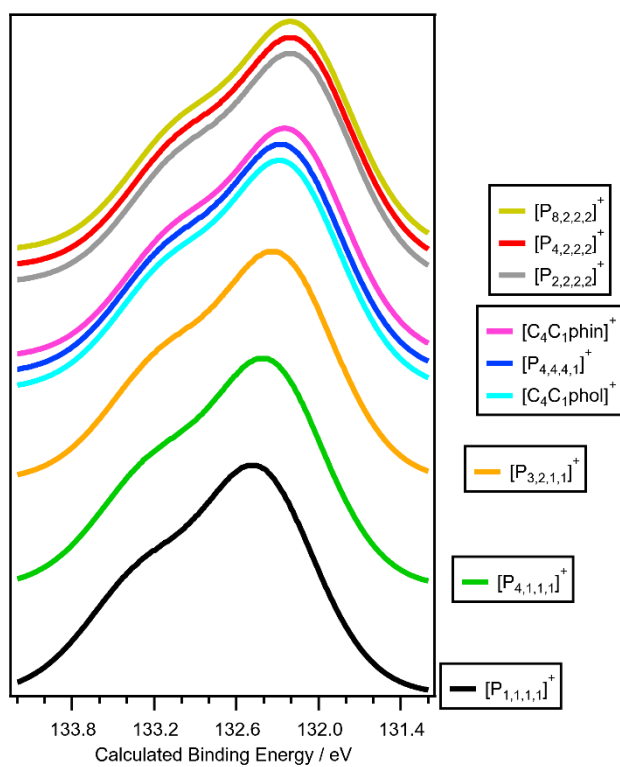


Figure S21. Calculated core P 2p, calc. XP spectra for: $[P_{1,1,1,1}]^+$, $[P_{4,1,1,1}]^+$, $[P_{3,2,1,1}]^+$, $[C_4C_1phin]^+$, $[P_{4,4,4,1}]^+$, $[C_4C_1phol]^+$, $[P_{8,2,2,2}]^+$, $[P_{4,2,2,2}]^+$, and $[P_{2,2,2,2}]^+$. Traces are vertically offset for clarity.

13. Effect of branching alkyl chains

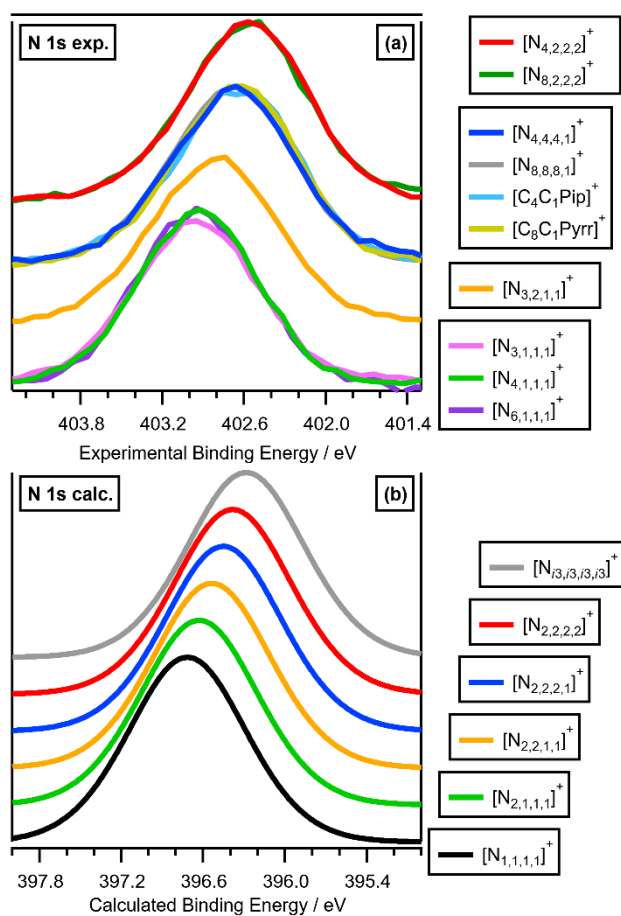


Figure S22. Experimental and calculated core XP spectra: (a) N 1s,exp. for $[N_{3,1,1,1}][NTf_2]$, $[N_{4,1,1,1}][NTf_2]$, $[N_{6,1,1,1}][NTf_2]$, $[N_{3,2,1,1}][NTf_2]$, $[N_{4,4,4,1}][NTf_2]$, $[N_{8,8,8,1}][NTf_2]$, $[C_4C_1Pip][NTf_2]$, $[C_8C_1Pyrr][NTf_2]$, $[N_{4,2,2,2}][NTf_2]$ and $[N_{8,2,2,2}][NTf_2]$; (b) N 1s,calc. for $[N_{1,1,1,1}]^+$, $[N_{2,1,1,1}]^+$, $[N_{2,2,1,1}]^+$, $[N_{2,2,2,1}]^+$, $[N_{2,2,2,2}]^+$ and $[N_{3,\beta,3,\beta}]^+$. Experimental XP spectra are area normalised and charge referenced using methods given in ESI Section 5. Traces are vertically offset for clarity.

14. Results. C 1s comparisons

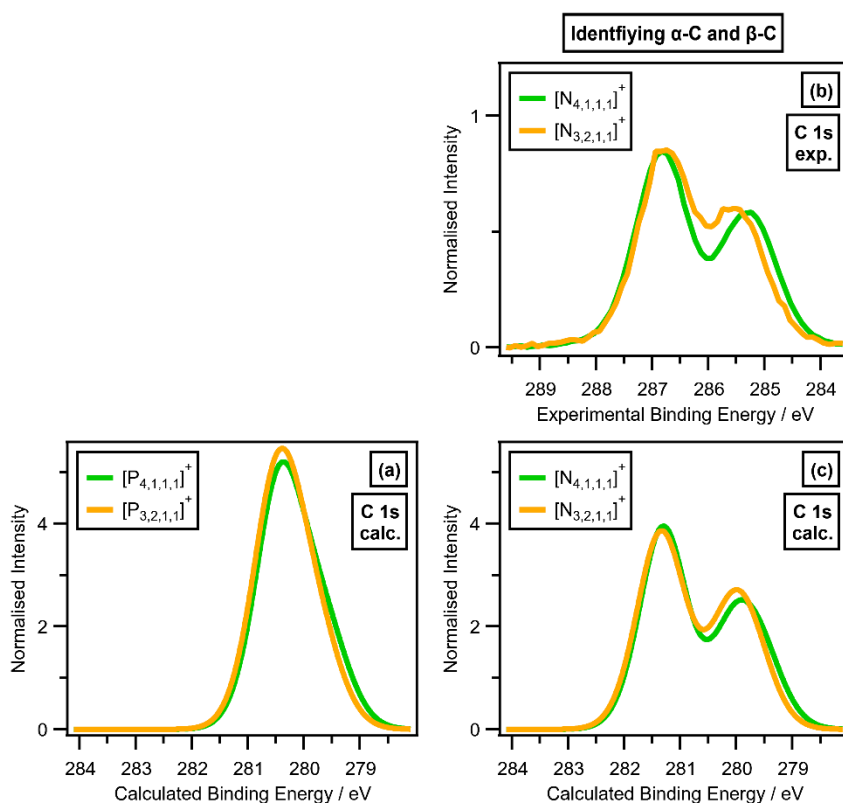


Figure S23. Experimental and calculated C 1s XP spectra: (a) C 1s,calc. for $[P_{4,1,1,1}]^+$ and $[P_{3,2,1,1}]^+$; (b) C 1s,exp. for $[N_{4,1,1,1}][NTf_2]$ and $[N_{3,2,1,1}][NTf_2]$ ionic liquids; (c) C 1s,calc. for $[N_{4,1,1,1}]^+$ and $[N_{3,2,1,1}]^+$; Experimental XP spectra are area normalised and charge referenced using methods given in ESI Section 5.

$E_B(\alpha\text{-C } 1s)$ show little variation when the alkyl chain length is varied when X is the same, with experimental $E_B(C_{N-C} 1s)$ the same for: $[N_{4,1,1,1}]^+$ and $[N_{4,2,2,2}]^+$ (Figure S24a and S24b); $[N_{3,2,1,1}]^+$ and $[N_{4,1,1,1}]^+$ (Figure S24c and S24d); $[N_{4,4,4,1}]^+$ and $[N_{8,8,8,1}]^+$ (Figure S25a and S25b); $[N_{3,1,1,1}]^+$, $[N_{4,1,1,1}]^+$ and $[N_{6,1,1,1}]^+$ (Figure S25c and S25d); $[N_{4,2,2,2}]^+$ and $[N_{8,2,2,2}]^+$ (Figure S25e and S25f); $[N_{4,1,1,1}]^+$ and $[N_{4,4,4,1}]^+$ (Figure S26a and S26b); $[S_{2,2,1}]^+$ and $[S_{2,2,2}]^+$ (Figure S27a and S27b).

Contributions due to β -carbons can be readily identified at intermediate $E_B(C 1s)$ and V_C values by comparing $[N_{4,1,1,1}]^+$ versus $[N_{4,2,2,2}]^+$ (Figure S24a and S24b), where the extra carbon signal for $[N_{4,2,2,2}]^+$ over $[N_{4,1,1,1}]^+$ represents contributions from three extra β -carbons.

Increasing the alkyl chain length from $n \geq 2$ to longer gave the expected increase in relative intensity in the $E_B(C_{alkyl} 1s)$ region at small E_B and small V_C , as can clearly be seen for $[N_{n,n,n,1}]^+$ (where $n = 4$ and 8, Figure S25a and S25b), $[N_{n,1,1,1}]^+$ ($n = 3, 4$ and 6, Figure S25c and S25d) and $[N_{n,2,2,2}]^+$ ($n = 4$ and 8, Figure S25e and S25f).

Not all $E_B(C_{alkyl} 1s)$ are the same, as can clearly be seen for $[N_{n,n,n,1}]^+$ (where $n = 4$ and 8, Figure S25a and S25b), $[N_{n,1,1,1}]^+$ ($n = 3, 4$ and 6, Figure S25c and S25d) and $[N_{n,2,2,2}]^+$ ($n = 4$ and 8, Figure S25e and S25f), where the longer alkyl chain gives smaller $E_B(C_{alkyl} 1s)$.

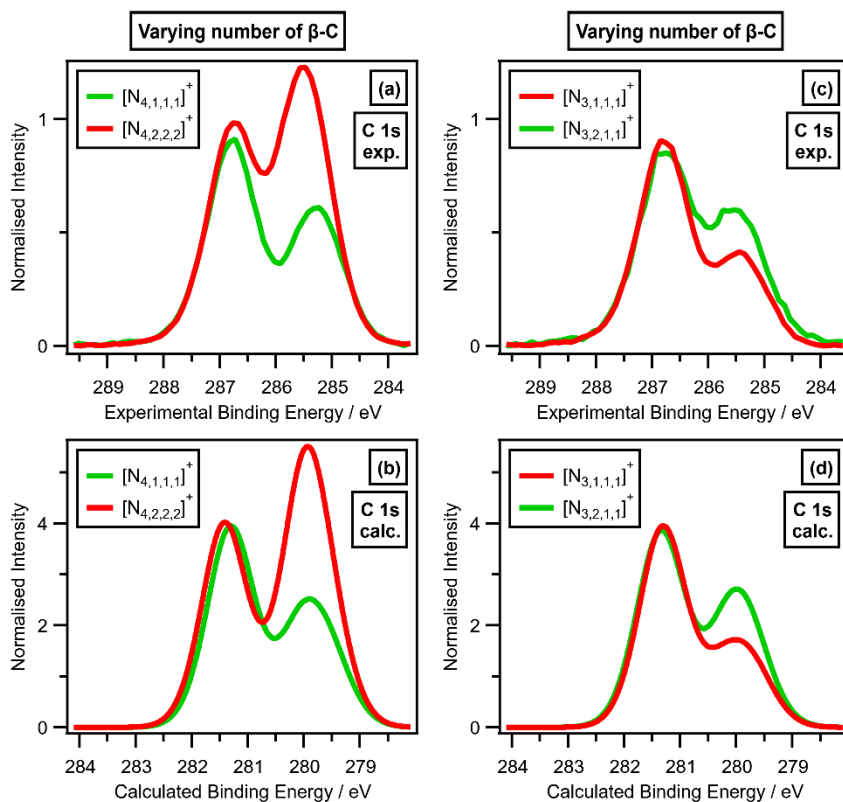


Figure S24. Experimental and calculated C 1s XP spectra: (a) C 1s,exp. for $[N_{4,1,1,1}]^+$ and $[N_{4,2,2,2}]^+$ ionic liquids; (b) C 1s,calc. for $[N_{4,1,1,1}]^+$ and $[N_{4,2,2,2}]^+$; (c) C 1s,exp. for $[N_{3,1,1,1}]^+$ and $[N_{3,2,1,1}]^+$ ionic liquids; (d) C 1s,calc. for $[N_{3,1,1,1}]^+$ and $[N_{3,2,1,1}]^+$. Experimental XP spectra are area normalised and charge referenced using methods given in ESI Section 5. Traces are vertically offset for clarity.

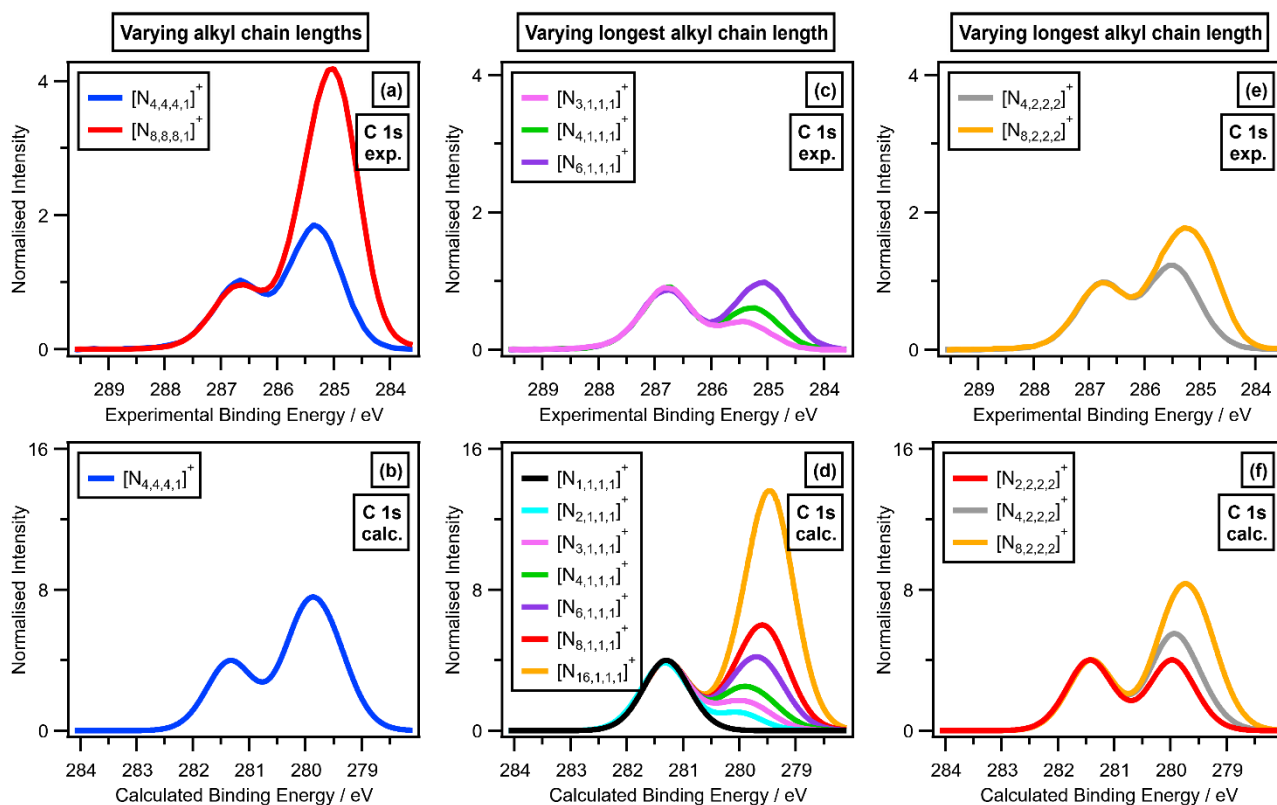


Figure S25. Experimental and calculated C 1s XP spectra: (a) C 1s,exp. for $[N_{4,4,4,1}]^+$ and $[N_{8,8,8,1}]^+$ ionic liquids; (b) C 1s,calc. for $[N_{4,4,4,1}]^+$; (c) C 1s,exp. for $[N_{3,1,1,1}]^+$, $[N_{4,1,1,1}]^+$ and $[N_{6,1,1,1}]^+$ ionic liquids; (d) C 1s,calc. for $[N_{1,1,1,1}]^+$, $[N_{2,1,1,1}]^+$, $[N_{3,1,1,1}]^+$, $[N_{4,1,1,1}]^+$, $[N_{6,1,1,1}]^+$, $[N_{8,1,1,1}]^+$, $[N_{16,1,1,1}]^+$; (e) C 1s,exp. for $[N_{4,2,2,2}]^+$ and $[N_{8,2,2,2}]^+$ ionic liquids; (f) C 1s,calc. for $[N_{2,2,2,2}]^+$, $[N_{4,2,2,2}]^+$ and $[N_{8,2,2,2}]^+$. Experimental XP spectra are area normalised and charge referenced using methods given in ESI Section 5. Traces are vertically offset for clarity.

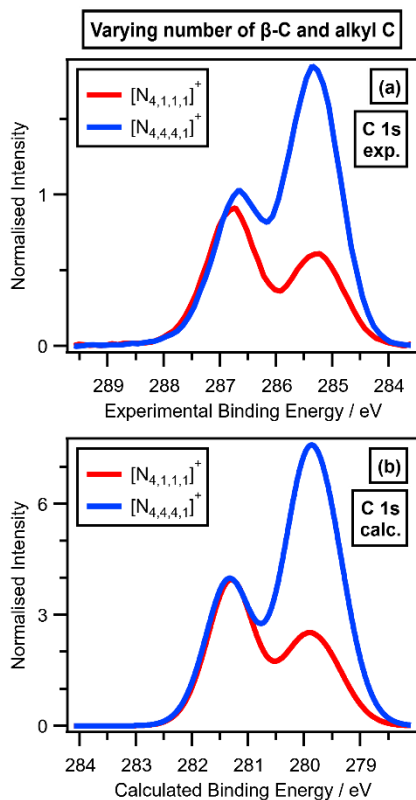


Figure S26. Experimental and calculated C 1s XP spectra: (a) C 1s,exp. for $[N_{4,1,1,1}][NTf_2]$ and $[N_{4,4,4,1}][NTf_2]$ ionic liquids; (b) C 1s,calc. for $[N_{4,1,1,1}]^+$ and $[N_{4,4,4,1}]^+$. Experimental XP spectra are area normalised and charge referenced using methods given in ESI Section 5.

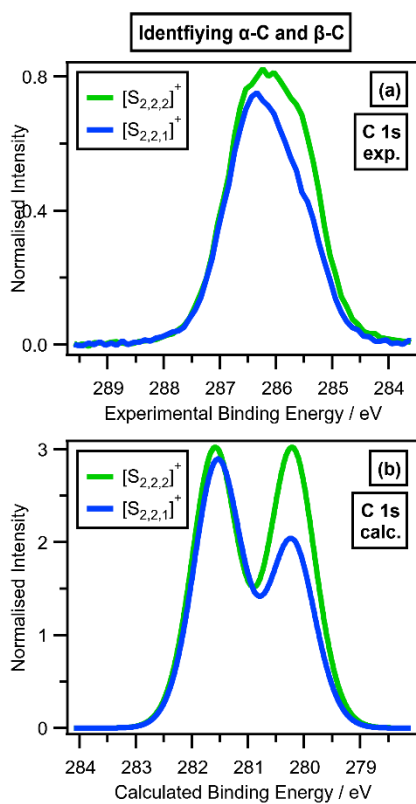


Figure S27. Experimental and calculated C 1s XP spectra: (a) C 1s,exp. for $[S_{2,2,1}][NTf_2]$ and $[S_{2,2,2}][NTf_2]$ ionic liquids; (b) C 1s,calc. for $[S_{2,2,1}]^+$ and $[S_{2,2,2}]^+$. Experimental XP spectra are area normalised and charge referenced using methods given in ESI Section 5.

15. References

1. D. C. Grinter, P. Ferrer, F. Venturini, M. A. van Spronsen, A. I. Large, S. Kumar, M. Jaugstetter, A. Iordachescu, A. Watts, S. L. M. Schroeder, A. Kroner, F. Grillo, S. M. Francis, P. B. Webb, M. Hand, A. Walters, M. Hillman and G. Held, *J. Synchrotron Radiat.*, 2024, **31**, 578-589.
2. R. M. Fogarty, R. G. Palgrave, R. A. Bourne, K. Handrup, I. J. Villar-Garcia, D. J. Payne, P. A. Hunt and K. R. J. Lovelock, *Phys. Chem. Chem. Phys.*, 2019, **21**, 18893-18910.
3. C. Kolbeck, M. Killian, F. Maier, N. Paape, P. Wasserscheid and H. P. Steinrück, *Langmuir*, 2008, **24**, 9500-9507.
4. M. J. Frisch, G. W. Trucks, H. B. Schlegel, G. E. Scuseria, M. A. Robb, J. R. Cheeseman, G. Scalmani, V. Barone, G. A. Petersson, H. Nakatsuji, X. Li, M. Caricato, A. V. Marenich, J. Bloino, B. G. Janesko, R. Gomperts, B. Mennucci, H. P. Hratchian, J. V. Ortiz, A. F. Izmaylov, J. L. Sonnenberg, D. Williams-Young, F. Ding, F. Lipparini, F. Egidi, J. Goings, B. Peng, A. Petrone, T. Henderson, D. Ranasinghe, V. G. Zakrzewski, J. Gao, N. Rega, G. Zheng, W. Liang, M. Hada, M. Ehara, K. Toyota, R. Fukuda, J. Hasegawa, M. Ishida, T. Nakajima, Y. Honda, O. Kitao, H. Nakai, T. Vreven, K. Throssell, J. J. A. Montgomery, J. E. Peralta, F. Ogliaro, M. J. Bearpark, J. J. Heyd, E. N. Brothers, K. N. Kudin, V. N. Staroverov, T. A. Keith, R. Kobayashi, J. Normand, K. Raghavachari, A. P. Rendell, J. C. Burant, S. S. Iyengar, J. Tomasi, M. Cossi, J. M. Millam, M. Klene, C. Adamo, R. Cammi, J. W. Ochterski, R. L. Martin, K. Morokuma, O. Farkas, J. B. Foresman and D. J. Fox, *Journal*, 2016.
5. J. D. Chai and M. Head-Gordon, *J. Chem. Phys.*, 2008, **128**, 084106.
6. J. D. Chai and M. Head-Gordon, *Phys. Chem. Chem. Phys.*, 2008, **10**, 6615-6620.
7. F. Weigend and R. Ahlrichs, *Phys. Chem. Chem. Phys.*, 2005, **7**, 3297-3305.
8. F. Weigend, *Phys. Chem. Chem. Phys.*, 2006, **8**, 1057-1065.
9. V. S. Bernales, A. V. Marenich, R. Contreras, C. J. Cramer and D. G. Truhlar, *J. Phys. Chem. B*, 2012, **116**, 9122-9129.
10. J. M. Seymour, E. Gousseva, F. K. Towers Tompkins, L. G. Parker, N. O. Ablewi, C. J. Clarke, S. Hayama, R. G. Palgrave, R. A. Bennett, R. P. Matthews and K. R. J. Lovelock, *Faraday Discuss.*, 2024, DOI: 10.1039/D1034FD00029C.
11. M. Giesbers, A. T. M. Marcelis and H. Zuilhof, *Langmuir*, 2013, **29**, 4782-4788.
12. N. P. Bellafont, P. S. Bagus and F. Illas, *J. Chem. Phys.*, 2015, **142**, 214102.
13. M. W. D. Hanson-Heine, M. W. George and N. A. Besley, *J. Chem. Phys.*, 2019, **151**, 9.
14. C. J. Clarke, H. Baaqel, R. P. Matthews, Y. Y. Chen, K. R. J. Lovelock, J. P. Hallett and P. Licence, *Green Chem.*, 2022, **24**, 5800-5812.
15. R. M. Fogarty, R. P. Matthews, C. R. Ashworth, A. Brandt-Talbot, R. G. Palgrave, R. A. Bourne, T. V. Hoogerstraete, P. A. Hunt and K. R. J. Lovelock, *J. Chem. Phys.*, 2018, **148**, 193817.
16. R. M. Fogarty, R. Rowe, R. P. Matthews, M. T. Clough, C. R. Ashworth, A. Brandt, P. J. Corbett, R. G. Palgrave, E. F. Smith, R. A. Bourne, T. W. Chamberlain, P. B. J. Thompson, P. A. Hunt and K. R. J. Lovelock, *Faraday Discuss.*, 2018, **206**, 183-201.
17. J. M. Seymour, E. Gousseva, A. I. Large, C. J. Clarke, P. Licence, R. M. Fogarty, D. A. Duncan, P. Ferrer, F. Venturini, R. A. Bennett, R. G. Palgrave and K. R. J. Lovelock, *Phys. Chem. Chem. Phys.*, 2021, **23**, 20957-20973.
18. F. K. Towers Tompkins, L. G. Parker, R. M. Fogarty, E. Gousseva, J. M. Seymour, C. J. Clarke, R. Seidel, R. Rowe, R. G. Palgrave, R. P. Matthews, R. A. Bennett, R. Grau-Crespo, P. A. Hunt and K. R. J. Lovelock, 2024, in preparation.
19. C. Kolbeck, T. Cremer, K. R. J. Lovelock, N. Paape, P. S. Schulz, P. Wasserscheid, F. Maier and H. P. Steinrück, *J. Phys. Chem. B*, 2009, **113**, 8682-8688.